New Scaling Relations of Galaxy Cluster Radio Halos

Marco Balboni, *S. Ettori, F. Gastaldello, R. Cassano, A. Bonafede, V. Cuciti, A. Botteon et al. 2025,*
A&A, 695, A180

SKA Workshop - 27/11/2025

GCs multifrequency overview

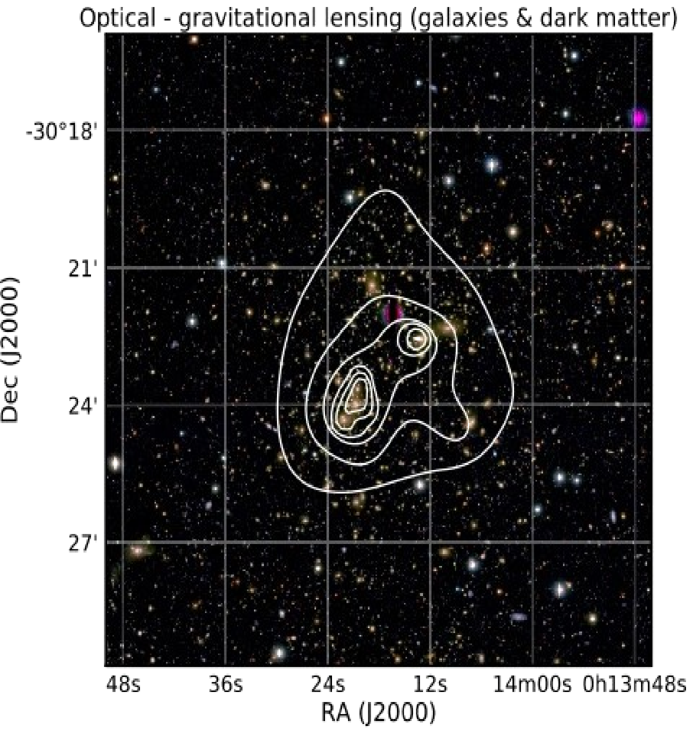

Clusters of galaxies are the largest objects in the Universe which are held together by their own gravity.

- Masses: $10^{14} - 10^{15}$ M_{sun} (~80% dark matter)
- Galaxies: 100s to 1000s
- Size: R~1 Mpc

GCs multifrequency overview

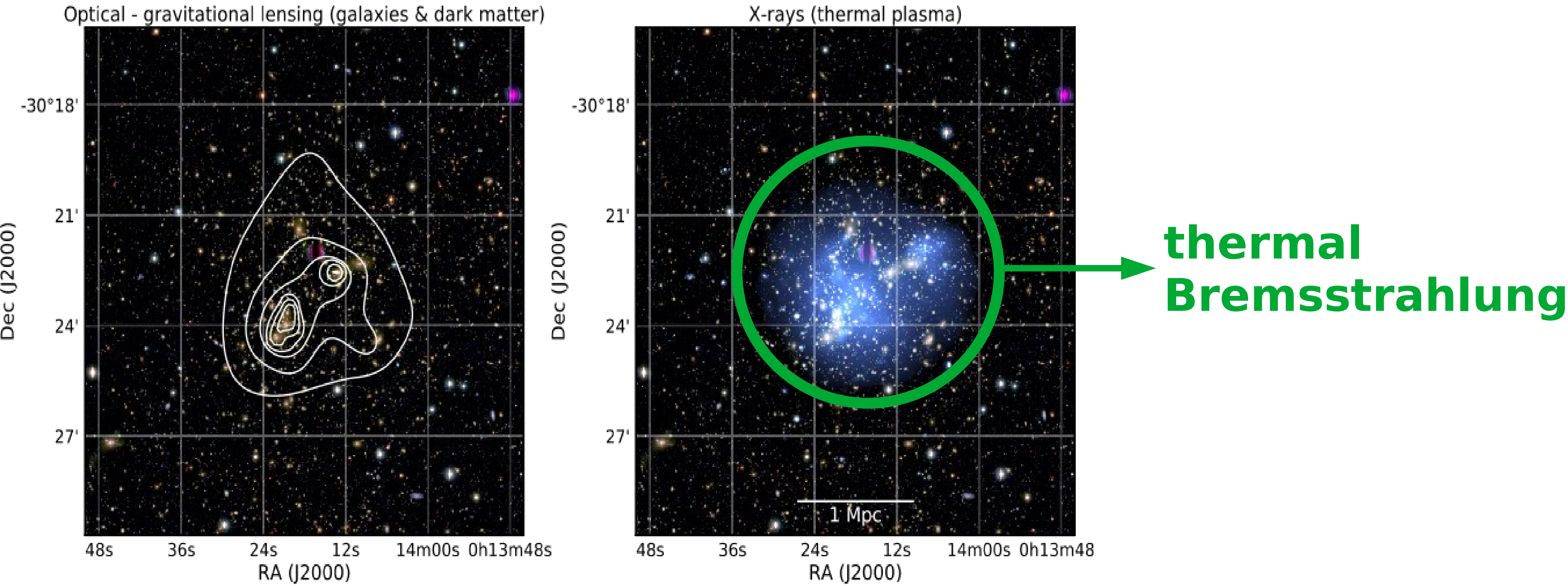

GCs multifrequency overview

Synchrotron (CRe$^-$ + weak B)

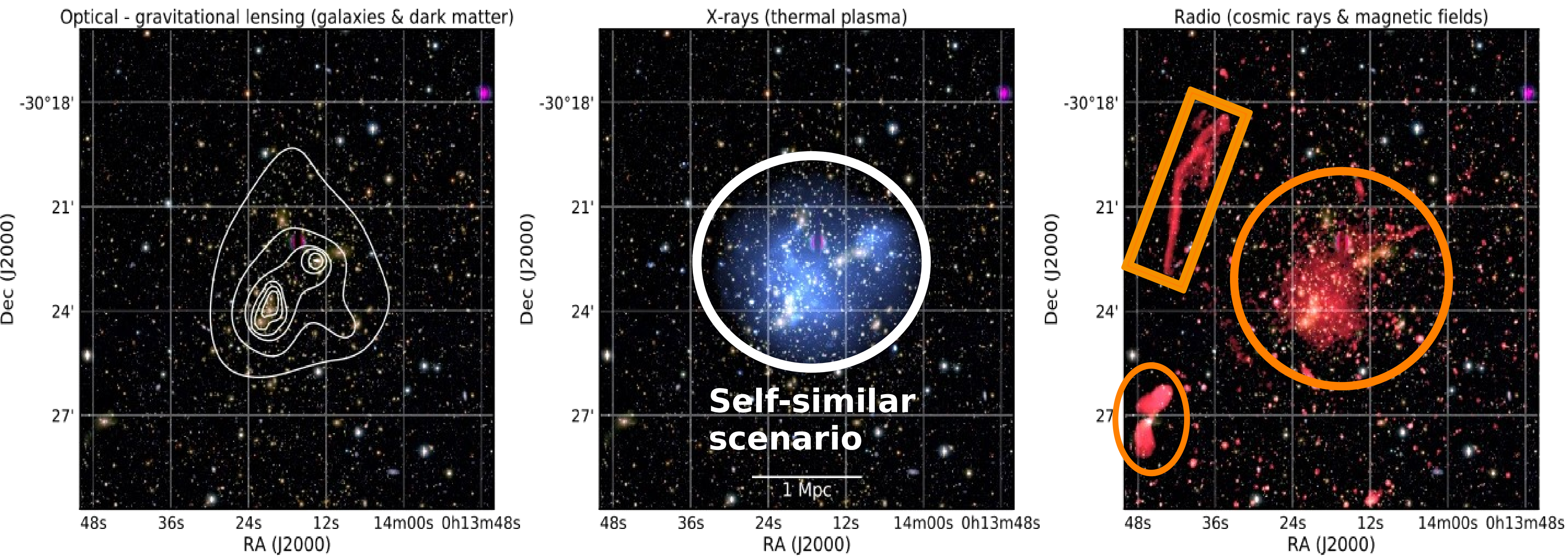

GCs multifrequency overview

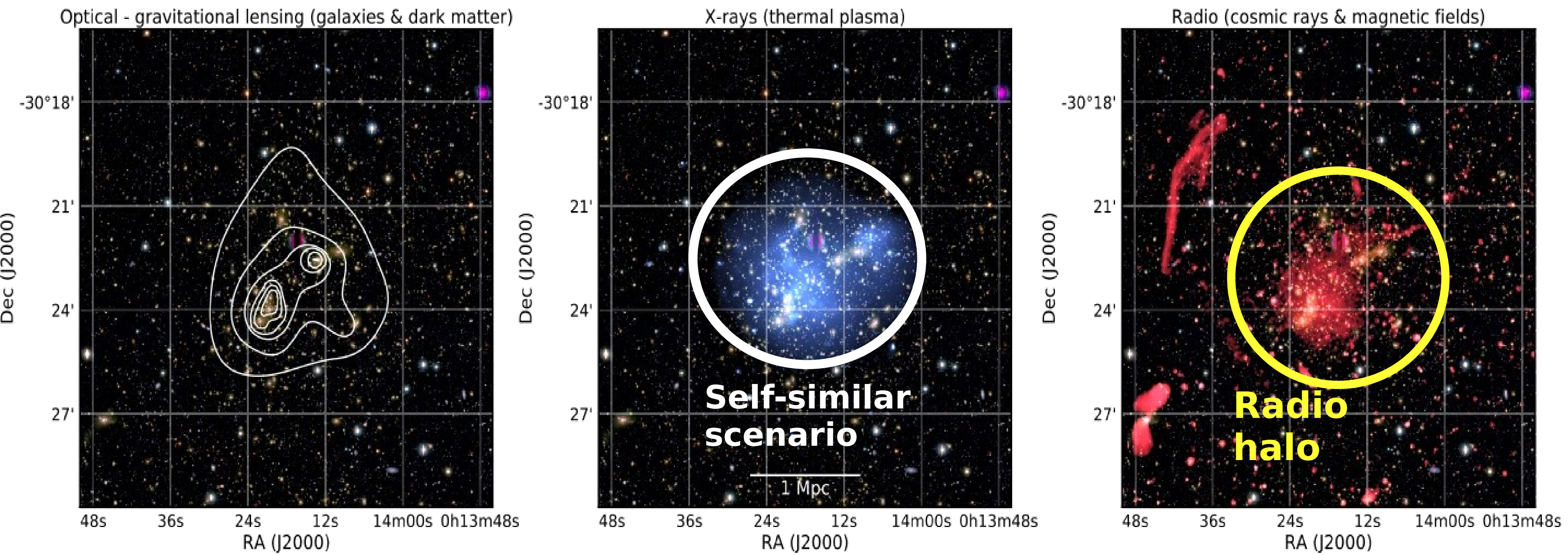

Self-similar scenario

- At cluster scales gravity dominates causing a self-similar evolution

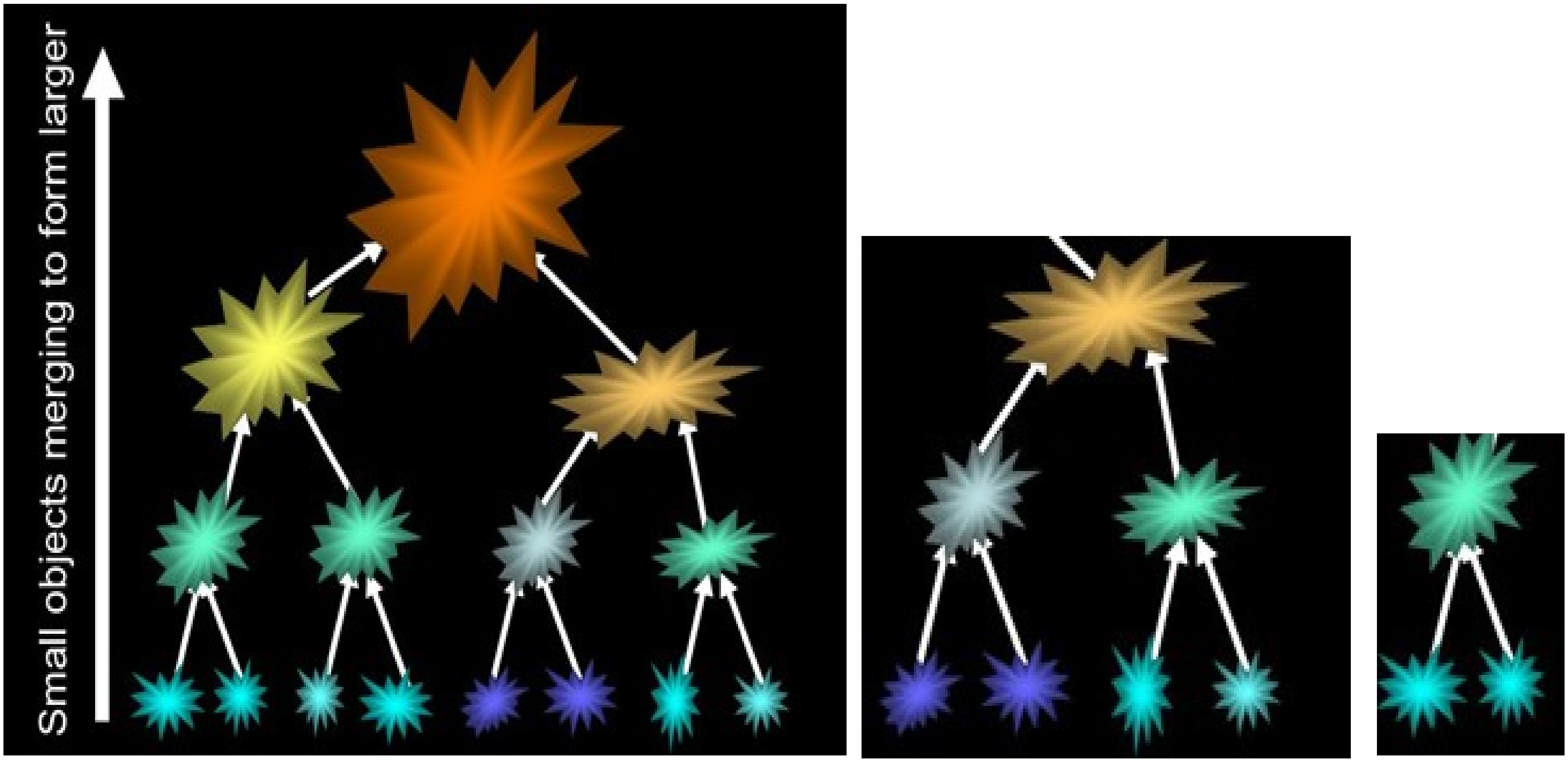

Credits: https://astronomy.swin.edu.au/cosmos/*/Hierarchical+Clustering

Self-similar scenario

- At cluster scales gravity dominates causing a self-similar evolution
- Well studied through X-ray observations of ICM:
  - Scaling relations among global properties, L_X – M, T – M, L_X – T (e.g. Pratt+09, Lovisari+2015) and resolved ones, ρ(r), T(r) (e.g. Arnaud+2010, Rossetti+24)

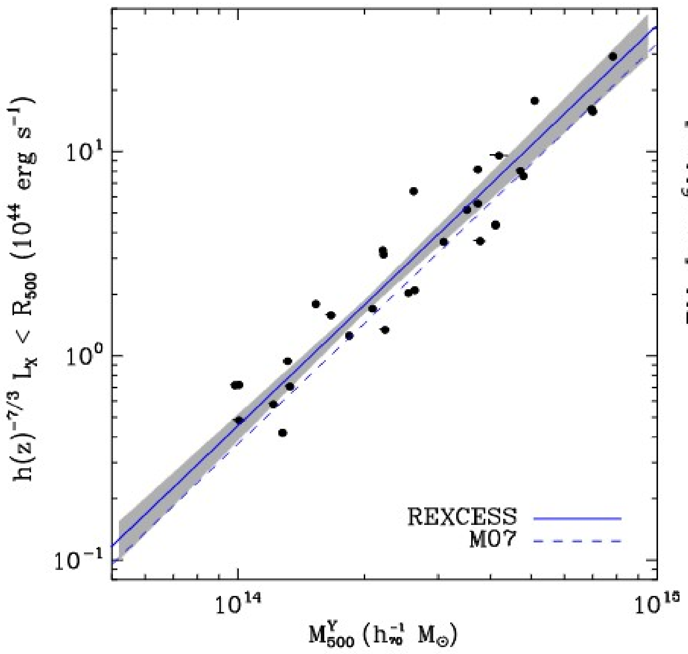

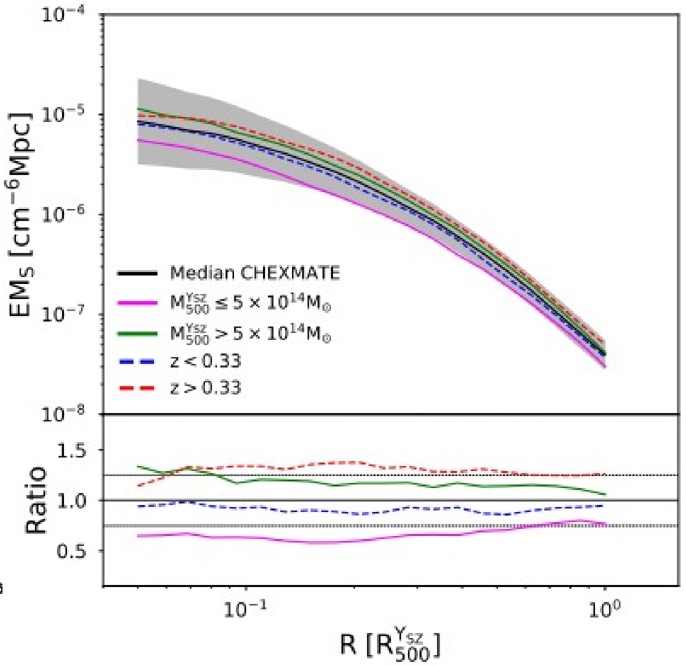

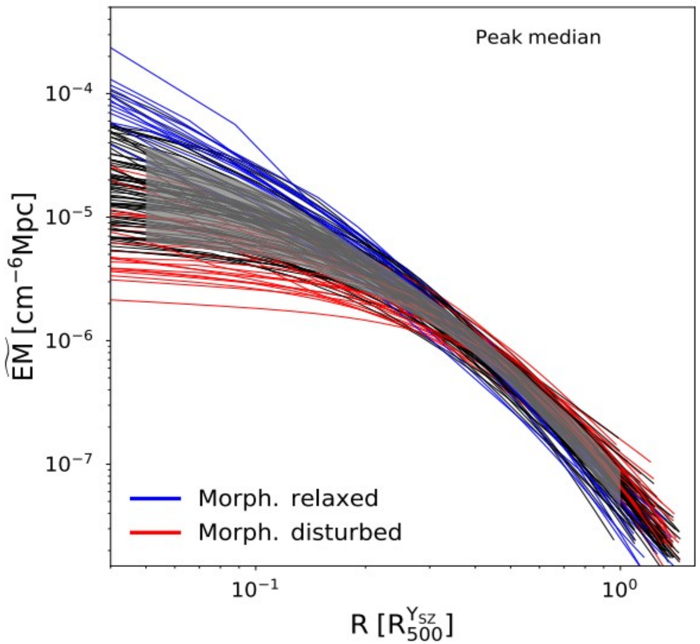

Scaling laws in radio

- Non-thermal component scaling relations have been studied for integrated quantities: $P_R - L_X$, P_R - M, $P_R - Y_{SZ,500}$ (e.g Cassano+13, Kale+15, Cuciti+23)

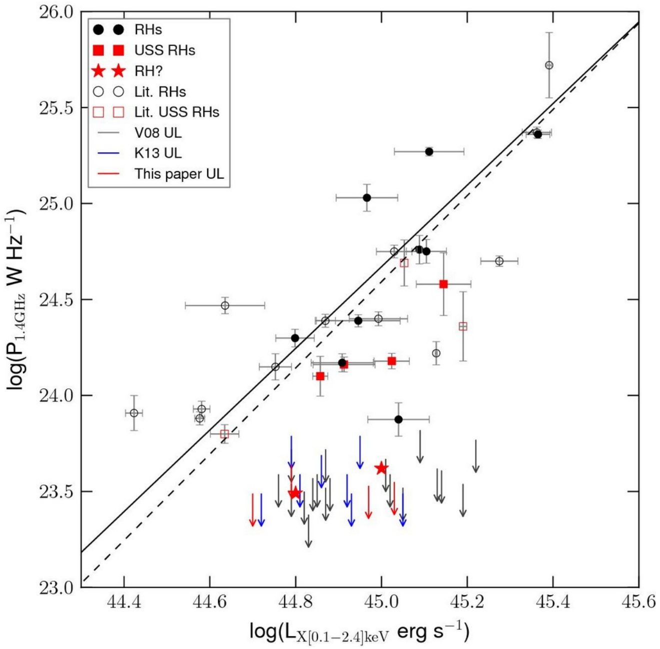

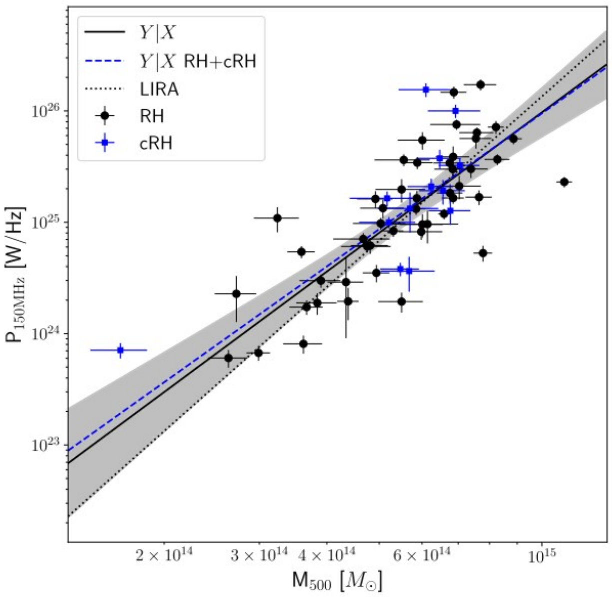

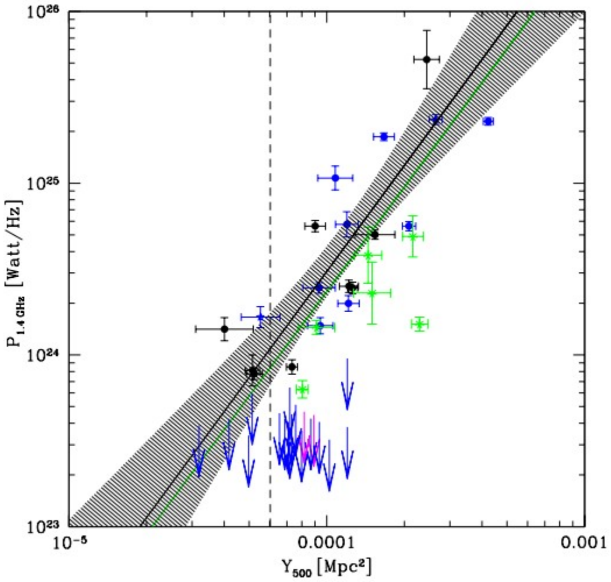

Scaling laws in radio

- Non-thermal component scaling relations have been studied for integrated quantities: $P_R – L_X$, P_R - M, $P_R – Y_{SZ,500}$ (e.g Cassano+13, Kale+15, Cuciti+23)

- No systematic studies have been made on the scaling of spatially resolved properties (but also on the P_R redshift dependence)

Datasets

UNIFORM DEPTH

CHEX-MATE

- Representative PSZ sample of 118 GC
- Homogeneous X-ray coverage
- Low and high redshift objects (Tier1 and Tier2)

Aims:

- Cluster absolute mass scale
- Cluster statistical properties
- How cluster properties changes over the time

CHEX-MATE Collaboration et al. 2021
Campitiello et al. 2022

LoTSS DR2

- Deep 120-168 MHz survey of the Northen sky
- High sensitivity (100 muJy/beam)
- Ideal for halos studies (83 so far)

Botteon et al. 2022
Bruno et al. 2023
Zhang et al. 2023
Cassano et al. 2023
Cuciti et al. 2023
Jones et al. 2023

Radio re-scaling

- Extracted the radial profiles from the 16 CHEX-MATE - LoTSS DR2 (z<0.4)

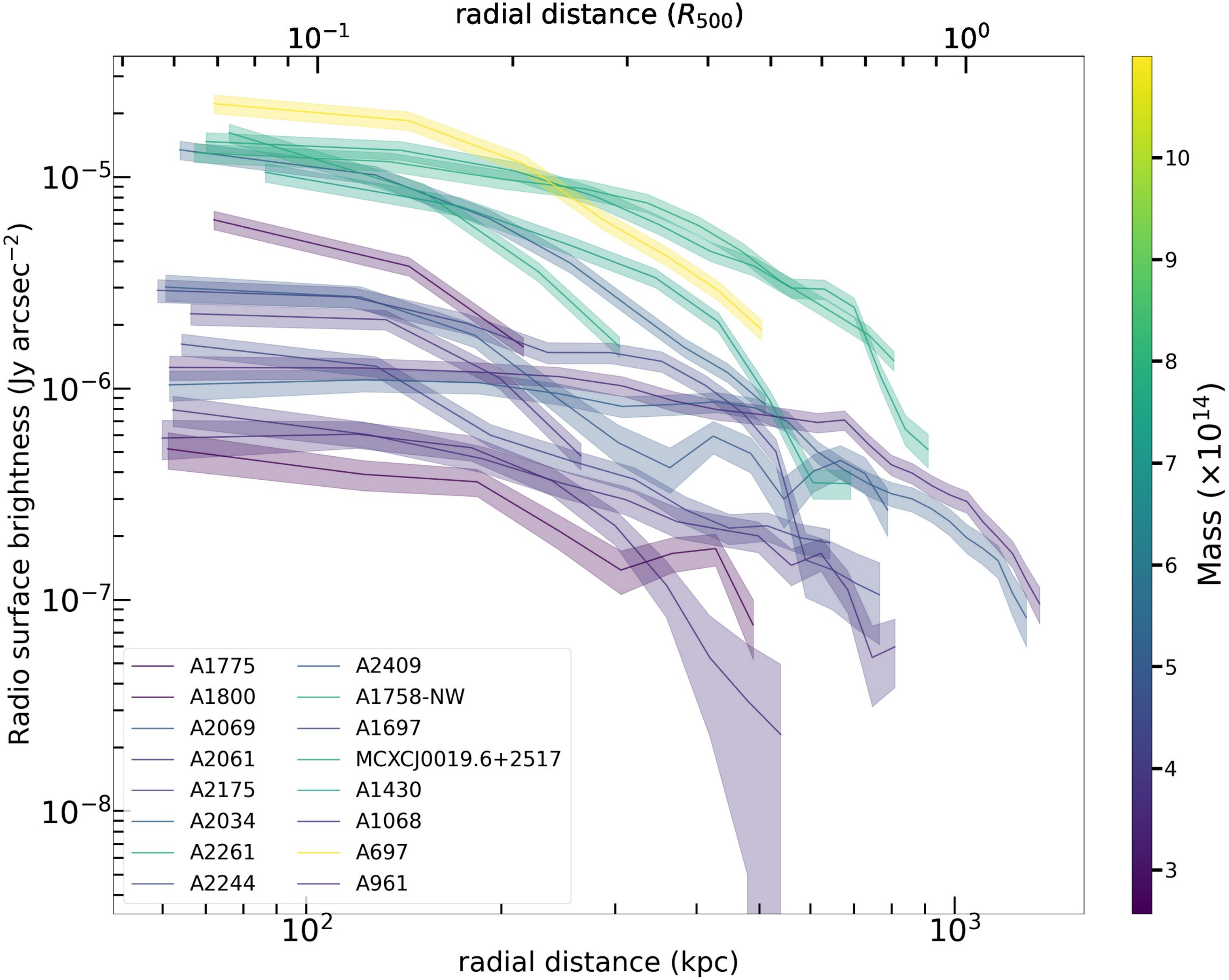

Radio re-scaling

- Extracted the radial profiles from the 16 CHEX-MATE - LoTSS DR2 (z<0.4)
- Derived the expected scaling in mass for the profiles assuming $R_H \sim M^{\beta} E_z^{\beta}$. Compared the mass expected dependence with the best-fit scaling

$$P_{150} = 4\pi D_L^2 \frac{S_{150}}{(1+z)^{\alpha+1}}$$

$$P_R \propto (M E_z)^{\alpha_M}$$

$$S_{150} \sim I_{150} R_{halo}^2 \left(\frac{D_L}{D_\theta}\right)^2 \sim I_{150} M^{-2\beta_M} E_z^{-2\beta_z} (1+z)^4$$

$$\boxed{I_{150}(r) \propto (M)^{\alpha_M - 2\beta_M} E_z^{\alpha_M - 2\beta_z} (1+z)^{-(3+\alpha)}}$$

Radio re-scaling

- Extracted the radial profiles from the 16 CHEX-MATE - LoTSS DR2 (z<0.4)
- Derived the expected scaling in mass for the profiles assuming $R_H \sim M^{\beta} E_z^{\beta}$. Compared the mass expected dependence with the best-fit scaling

$$P_{150} = 4\pi D_L^2 \frac{S_{150}}{(1+z)^{\alpha+1}}$$

$$P_R \propto (M E_z)^{\alpha_M}$$

$$S_{150} \sim I_{150} R_{halo}^2 \left(\frac{D_L}{D_\theta}\right)^2 \sim I_{150} M^{-2\beta_M} E_z^{-2\beta_z} (1+z)^4$$

$$\begin{aligned} I_{150}(r) &\propto (M)^{\alpha_M - 2\beta_M} E_z^{\alpha_M - 2\beta_z} (1+z)^{-(3+\alpha)} \\ &= I_0 e^{\left(-A\frac{r}{r_{500}}\right)} M^{\gamma_M} E_z^{\gamma_z} (1+z)^{-(3+\alpha)} \end{aligned}$$

Radio re-scaling

- Extracted the radial profiles from the 16 CHEX-MATE - LoTSS DR2 (z<0.4)
- Derived the expected scaling in mass for the profiles assuming $R_H \sim M^{\beta} E_z^{\beta}$. Compared the mass expected dependence with the best-fit scaling
- Exploited the Cuciti+23 RH sample to derive mass and redshift P_R dependence, and same for R_H

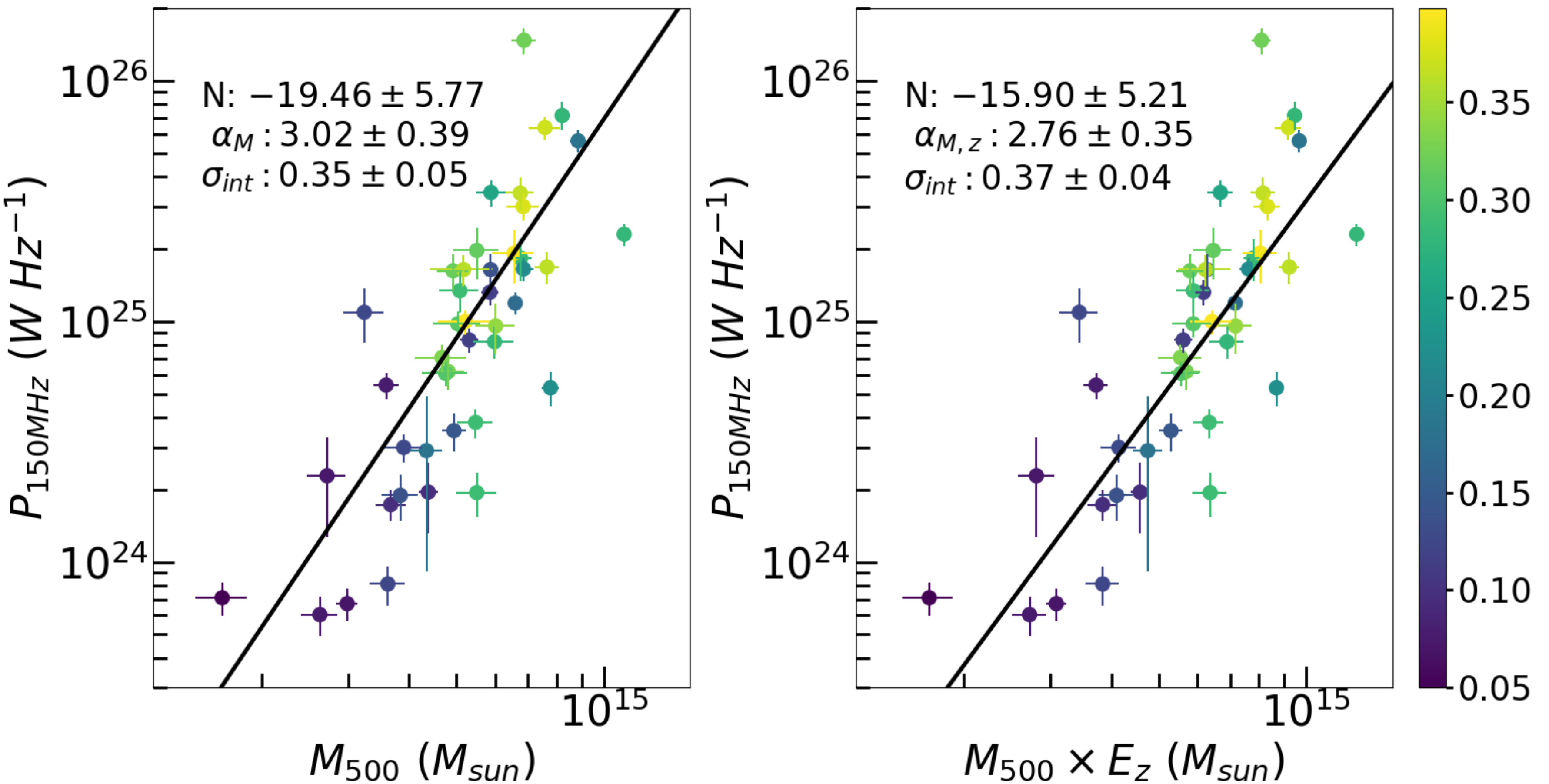

Radio re-scaling

- Extracted the radial profiles from the 16 CHEX-MATE - LoTSS DR2 (z<0.4)
- Derived the expected scaling in mass for the profiles assuming $R_H \sim M^{\beta} E_z^{\beta}$. Compared the mass expected dependence with the best-fit scaling
- Exploited the Cuciti+23 RH sample to derive mass and redshift P_R dependence, and same for R_H

$$R_H \propto M^{\beta_M} E_z^{\beta_z} \qquad \beta_M = 1/3, \beta_z = 0, -2/3 \qquad \rightarrow 0$$

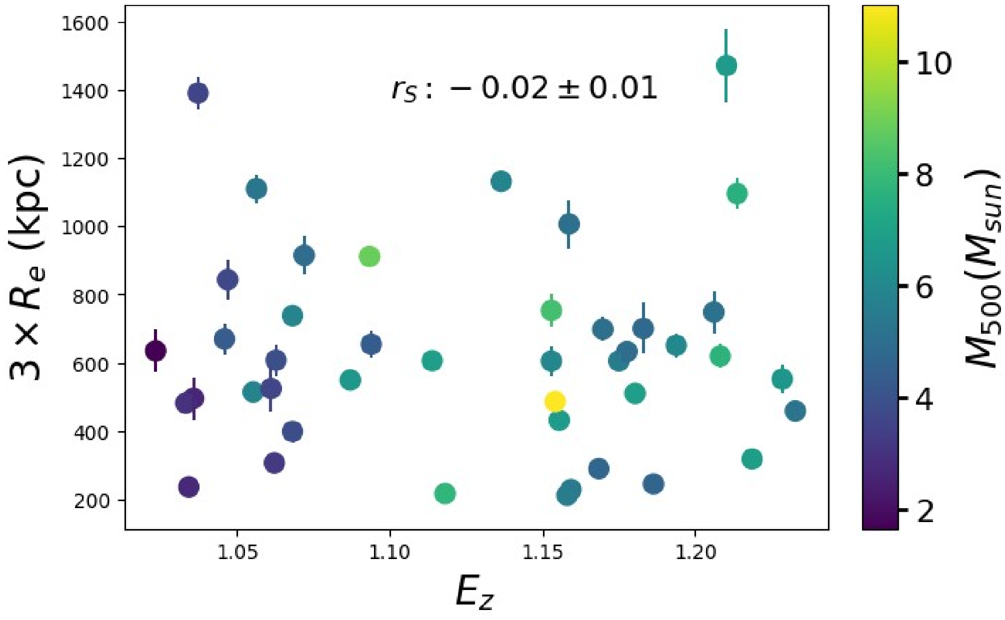

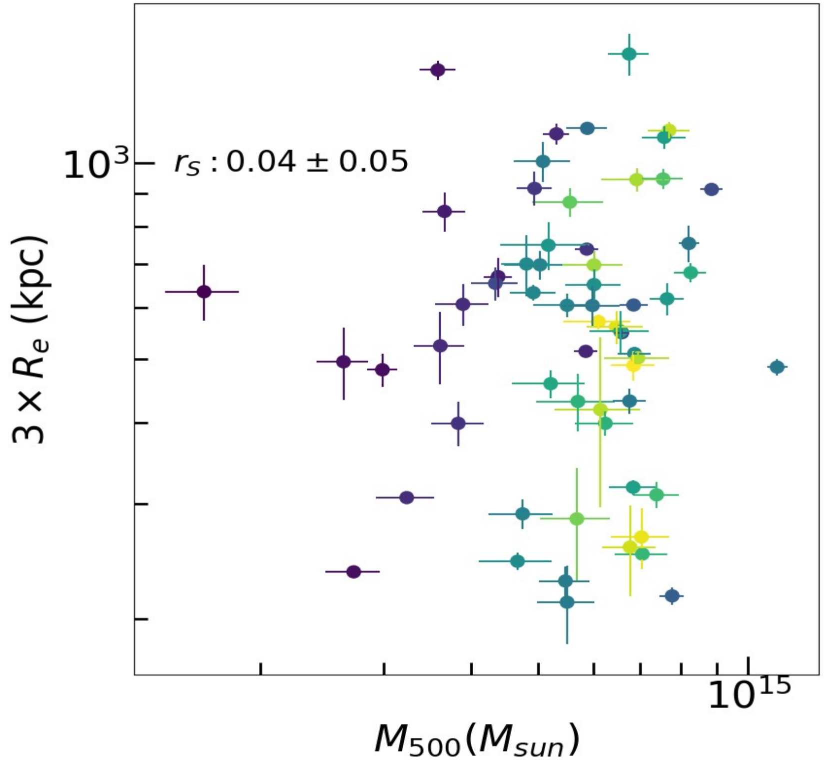

Radio re-scaling

	σ_{int}	Δ_σ	γ_M	$\Delta\,\gamma_M$	γ_z	$\Delta\,\gamma_z$
$I_{150MHz} \propto M^{\gamma_M}$	0.22	0.05	3.68	0.43	0 (fixed)	/
$I_{150MHz} \propto M^{\gamma_M}\ E_{z,\mathrm{fixed}}^{4/3}$	0.24	0.04	3.41	0.38	4/3 (fixed)	/
$I_{150MHz} \propto M^{\gamma_M}\ E_{z,\mathrm{fixed}}^{\alpha_M+4/3}$	0.28	0.04	2.85	0.43	4.10 (fixed)	/
$I_{150MHz} \propto (ME_z)^{\gamma_M}$	0.26	0.04	2.88	0.31	/	/

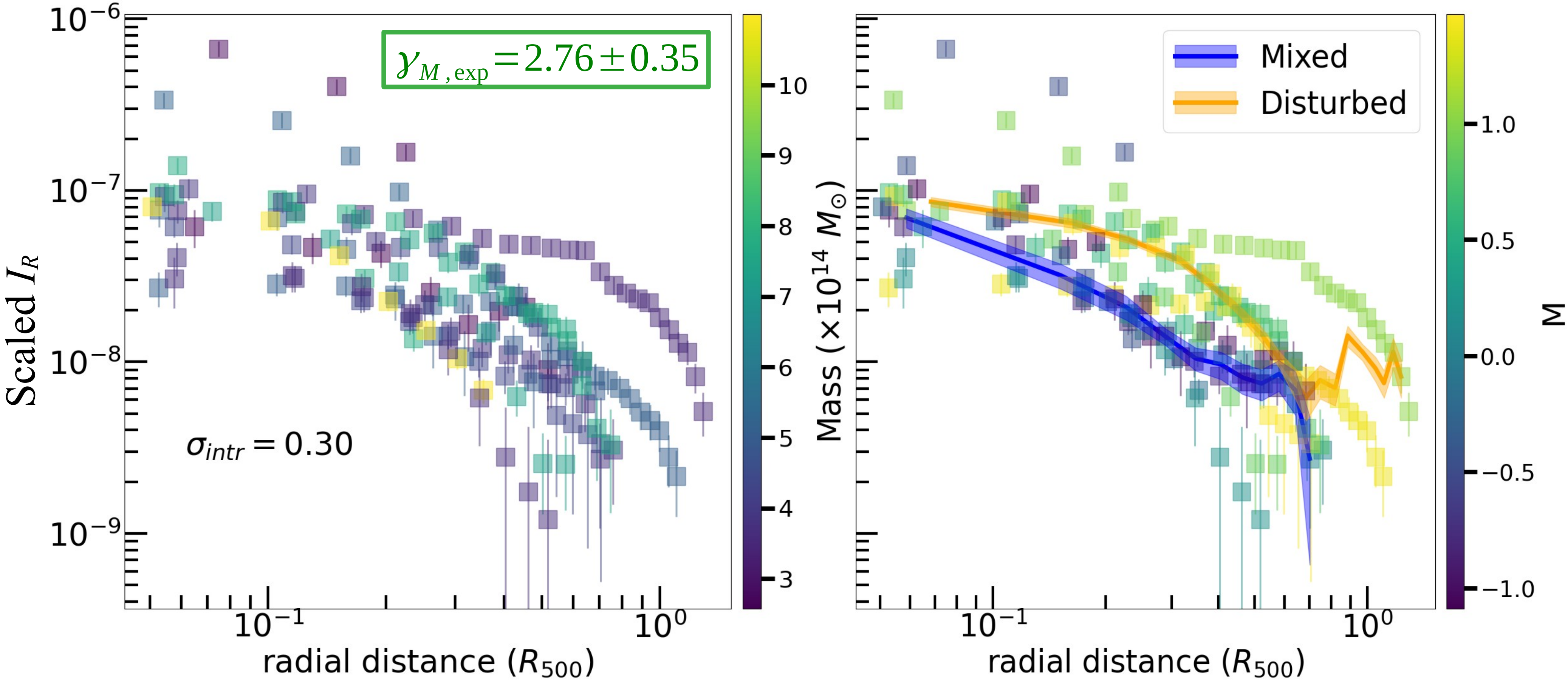

The role of B

The radio halo power

$$P_R = f(M, z)$$

In the context of turbulent re-acceleration (Cassano+05,06)

$$\boxed{P_R \propto M^{2-\Gamma} \frac{B^2 n_{e,r}}{(B^2 + B_{IC}^2)^2}}$$

If $B = B_{M'} \left(\frac{M}{M'} \right)^b$:

$$\boxed{\log(P_{150}) = N + \left(\frac{4}{3} - 2b \right) \log\left(\frac{M}{M'} \right) - 2\log\left[1 + \left(\frac{B_{CMB,0}}{B_{M'}} \right)^2 \frac{(1+z)^4}{(M/M')^{2b}} \right]}$$

The role of B

The radio halo power

$$P_R = f(M, z)$$

In the context of turbulent re-acceleration (Cassano+05,06)

$$\boxed{P_R \propto M^{2-\Gamma} \frac{B^2 n_{e,r}}{(B^2 + B_{IC}^2)^2}}$$

If $B = B_{M'} \left(\frac{M}{M'} \right)^b$:

$$\boxed{\log P_{150} = N + \left(\frac{4}{3} - 2b \right) \log \left(\frac{M}{M'} \right) - 2 \log \left[1 + \left(\frac{B_{CMB,0}}{B_{M'}} \right)^2 \frac{(1+z)^4}{(M/M')^{2b}} \right]}$$

The role of B

$$\log(P_{150}) = N + \left(\frac{4}{3} - 2b\right)\log\left(\frac{M}{M'}\right) - 2\log\left[1 + \left(\frac{B_{CMB,0}}{B_{M'}}\right)^2 \frac{(1+z)^4}{(M/M')^{2b}}\right]$$

Parameter	Prior	Best fit
b	$U(0, 10)$	2.05 ± 0.36
$B_{M'}$	$U(0, 10)$	2.53 ± 0.61
N	$U(0, 10)$	2.82 ± 0.83
σ_{int}	$HC(0.5)$	0.95 ± 0.13
b (fixed)	/	1.33
$B_{M'}$	$U(0, 10)$	2.11 ± 0.88
N	$U(0, 10)$	3.20 ± 1.69
σ_{int}	$HC(0.5)$	1.04 ± 0.13

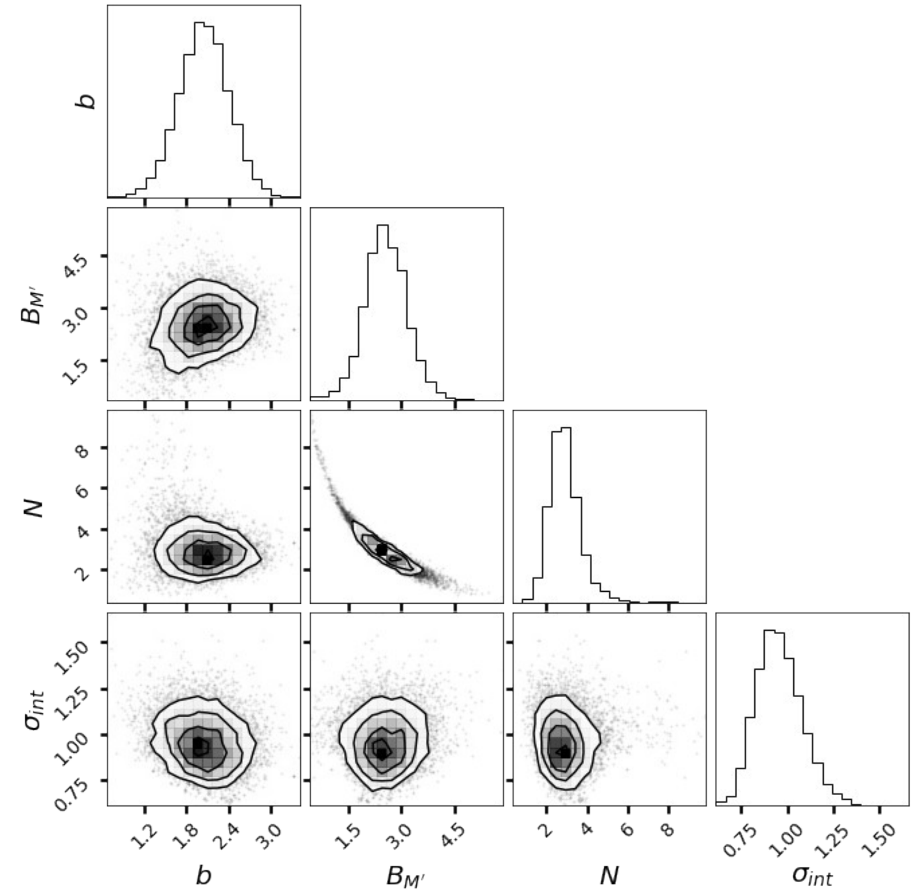

The role of B

$$\log(P_{150}) = N + \left(\frac{4}{3} - 2b\right)\log\left(\frac{M}{M'}\right) - 2\log\left[1 + \left(\frac{B_{CMB,0}}{B_{M'}}\right)^2 \frac{(1+z)^4}{(M/M')^{2b}}\right]$$

$$\alpha_M = \frac{\log(P_1/P_2)}{\log(M_1/M_2)} = \psi(b, B_{M'})$$

Constrained from the observed P-M relation

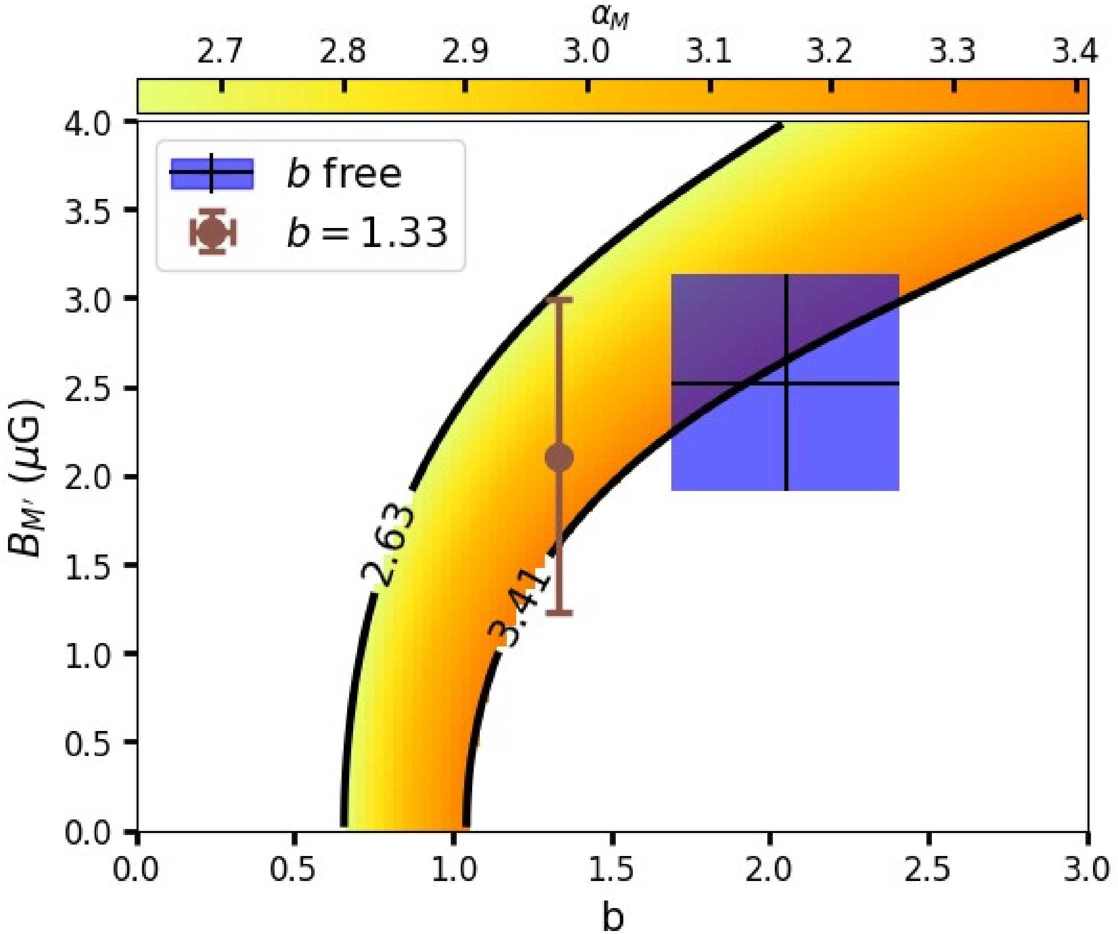

The role of B

$$\log(P_{150}) = N + \left(\frac{4}{3} - 2b\right)\log\left(\frac{M}{M'}\right) - 2\log\left[1 + \left(\frac{B_{CMB,0}}{B_{M'}}\right)^2 \frac{(1+z)^4}{(M/M')^{2b}}\right]$$

$$\alpha_M = \frac{\log(P_1/P_2)}{\log(M_1/M_2)} = \psi(b, B_{M'})$$

+

Parameter	Prior	Best fit
b	$U(0,10)$	2.05 ± 0.36
$B_{M'}$	$U(0,10)$	2.53 ± 0.61
N	$U(0,10)$	2.82 ± 0.83
σ_{int}	$HC(0.5)$	0.95 ± 0.13
b (fixed)	/	1.33
$B_{M'}$	$U(0,10)$	2.11 ± 0.88
N	$U(0,10)$	3.20 ± 1.69
σ_{int}	$HC(0.5)$	1.04 ± 0.13

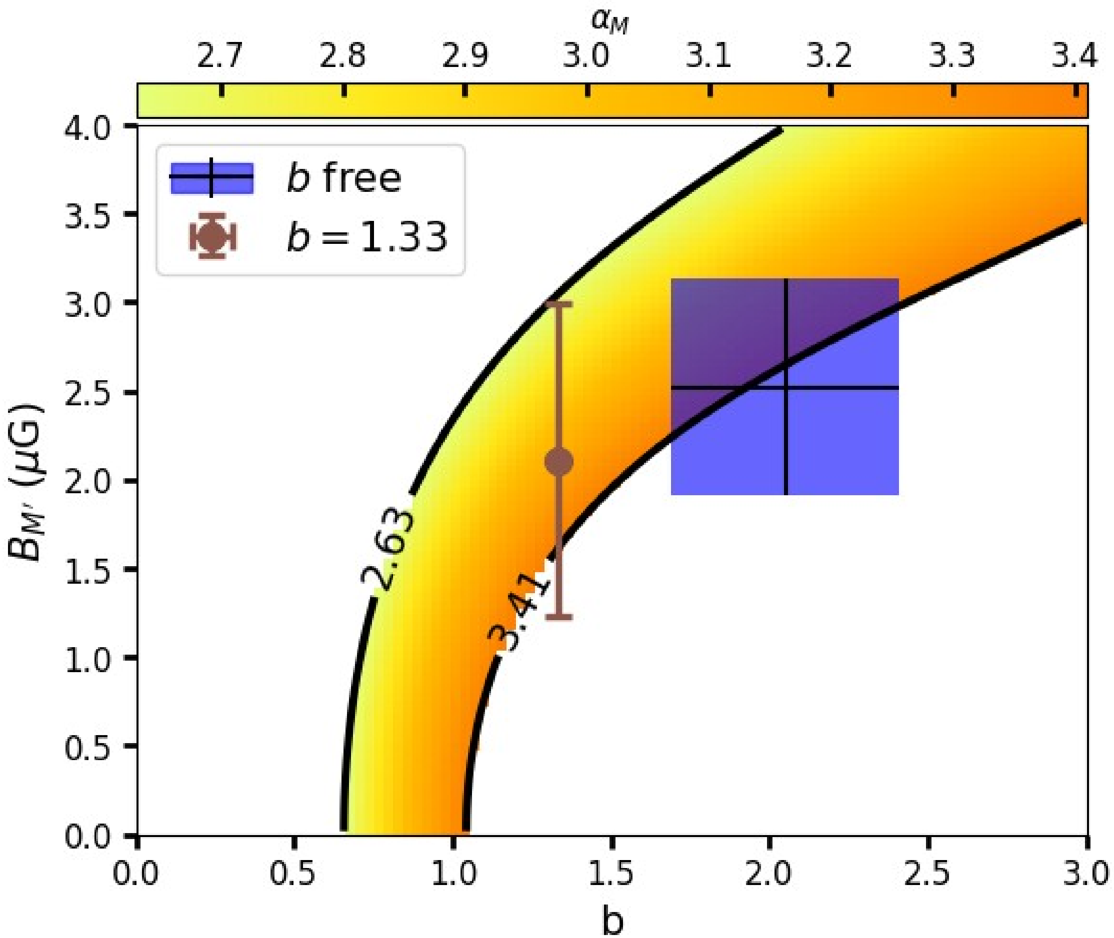

Summary

We studied the scaling properties of radio halo profiles finding:

- Strong cluster's mass depenced of the profiles from I_R-M(z) relation (no R_H role)
- The profile scatter to be singificantly reduced by M & z rescaling
- A residual dependence of the scaled profiles on the cluster dynamical state
- A strong (~2) mass dependence of the global cluster B

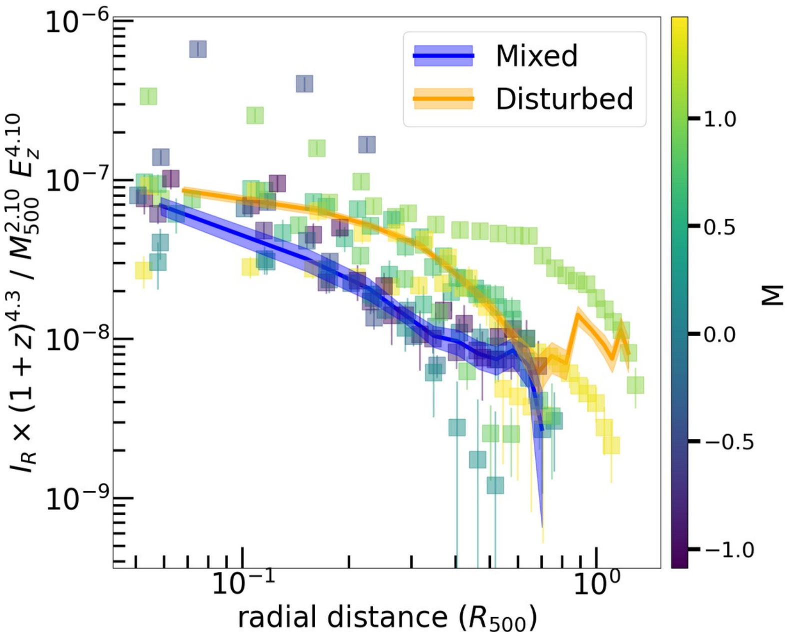

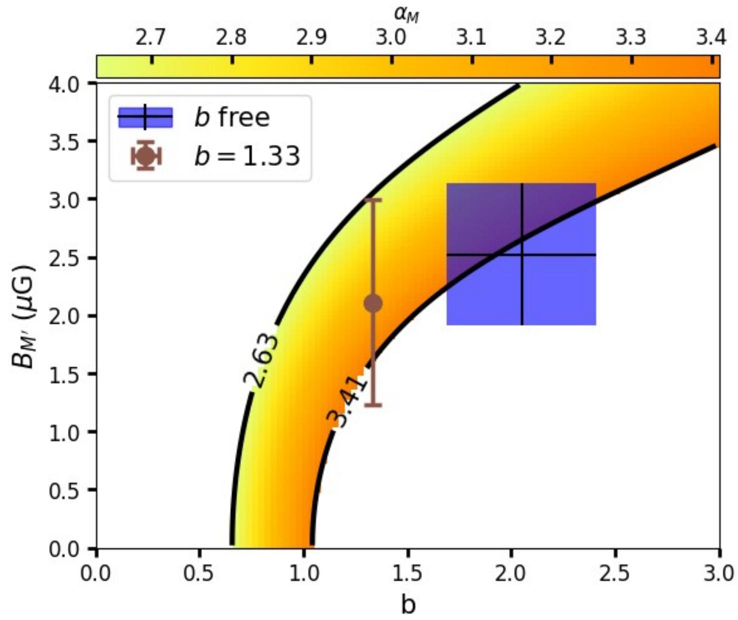

Future (SKA) prospects

Higher frequecies studies with MeerKAT:

- 36 massive (>7 x 10^{14} M_{sun}) CHEX-MATE objects
- All display diffuse radio emission
- Span a wide range of dynamical states
- Polarisation info (~20 already available)
- L + UHF band (274h + archive)

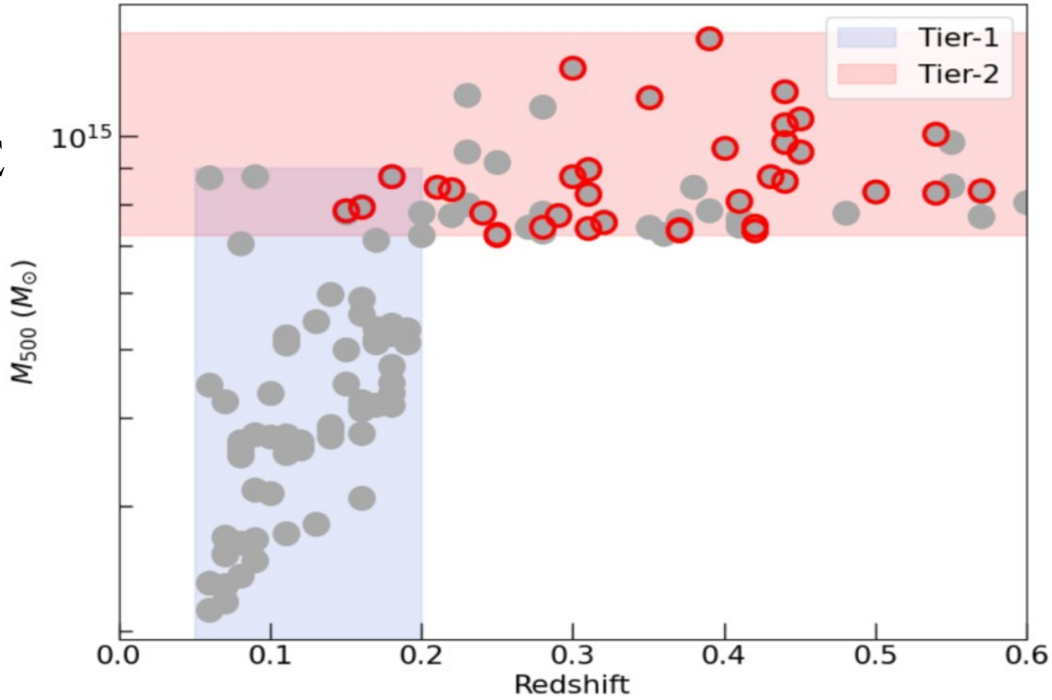

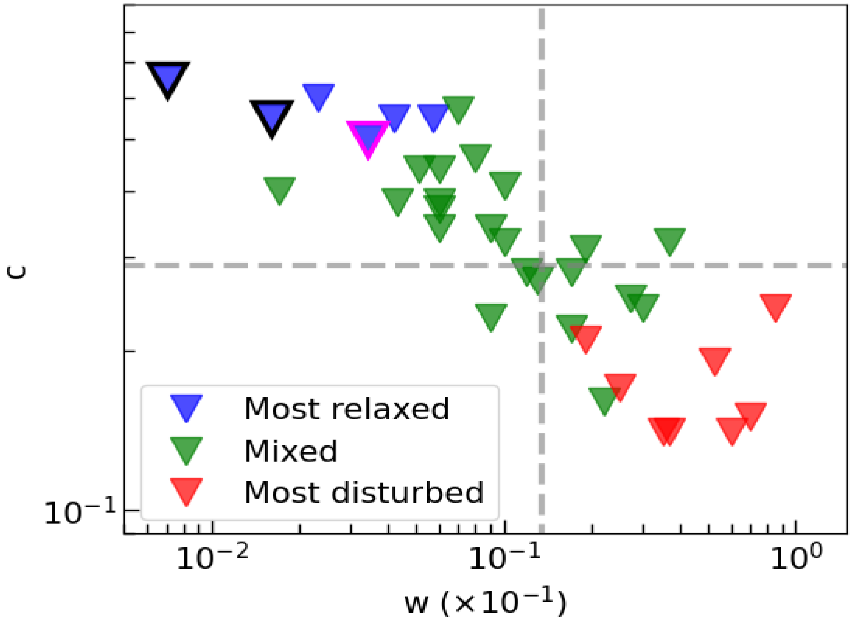

Future (SKA) prospects

Higher frequecies studies with MeerKAT:

- 36 massive (>7 x 10^{14} M_{sun}) CHEX-MATE objects
- All display diffuse radio emission
- Span a wide range of dynamical states
- Polarisation info (~20 already available)
- L + UHF band (274h + archive)

SKA-mid

SKA-low

LoTSS

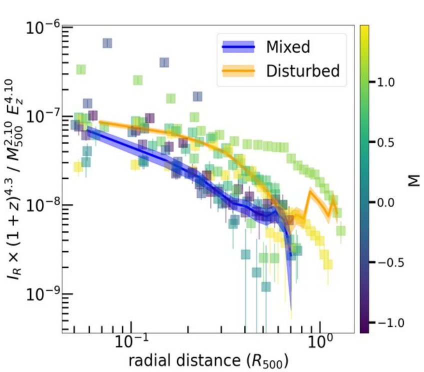

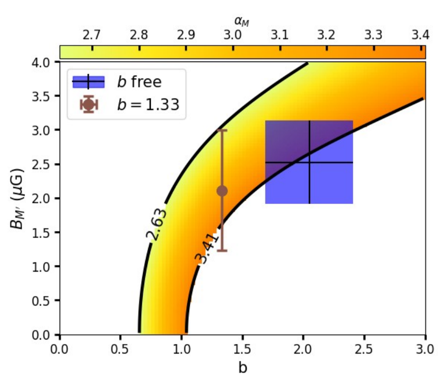

Summary

- We studied the scaling properties of radio halo profiles finding:
    - Strong cluster's mass depenced of the profiles from I_R-M(z) relation (no R_H role)
    - The profile scatter to be singificantly reduced by M & z rescaling
    - A residual dependence of the scaled profiles on the cluster dynamical state
    - A strong (~2) mass dependence of the global cluster B
- Forthcoming MeerKAT studies will provide further insights on the halo nature and pave the path for SKA-low & mid synergies

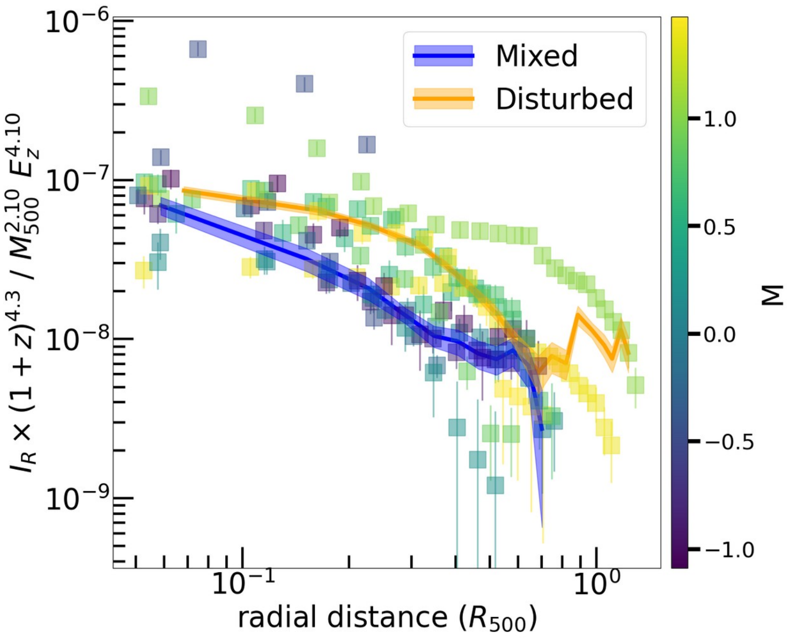

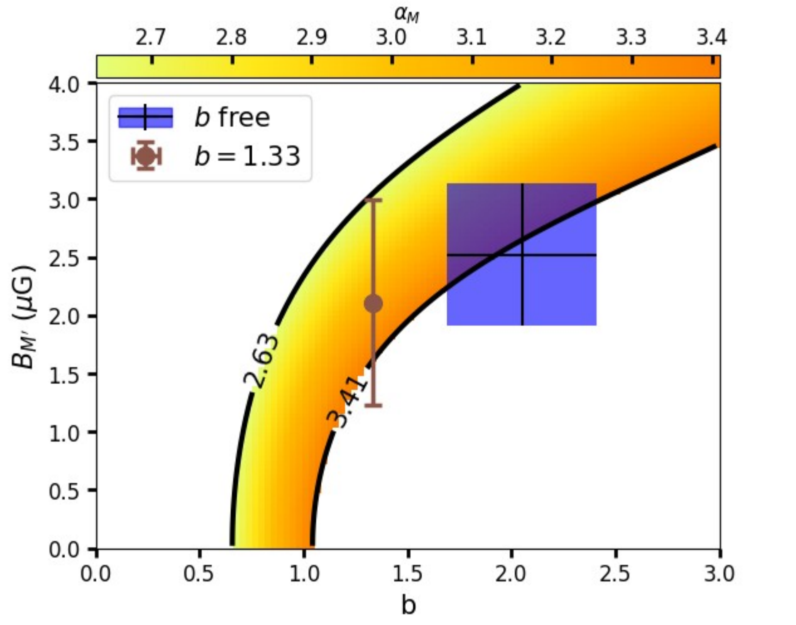

Thank you for the attention!

Radio re-scaling

$\gamma_{M,\exp}=2.10\pm0.35$ $\gamma_{M,\exp}=2.35\pm0.39$

	σ_{int}	Δ_σ	γ_M	$\Delta\gamma_M$	γ_z	$\Delta\gamma_z$
$I_{150MHz}\propto M^{\gamma_M}$	0.22	0.05	3.68	0.43	0 (fixed)	/
$I_{150MHz}\propto M^{\gamma_M}\,E_{z,\text{fixed}}^{4/3}$	0.24	0.04	3.41	0.38	4/3 (fixed)	/
$I_{150MHz}\propto M^{\gamma_M}\,E_{z,\text{fixed}}^{\alpha_M+4/3}$	0.28	0.04	2.85	0.43	4.10 (fixed)	/

$$R_H\propto M^{\beta_M}E_z^{\beta_z}\qquad \beta_M=1/3,\beta_z=0,-2/3$$

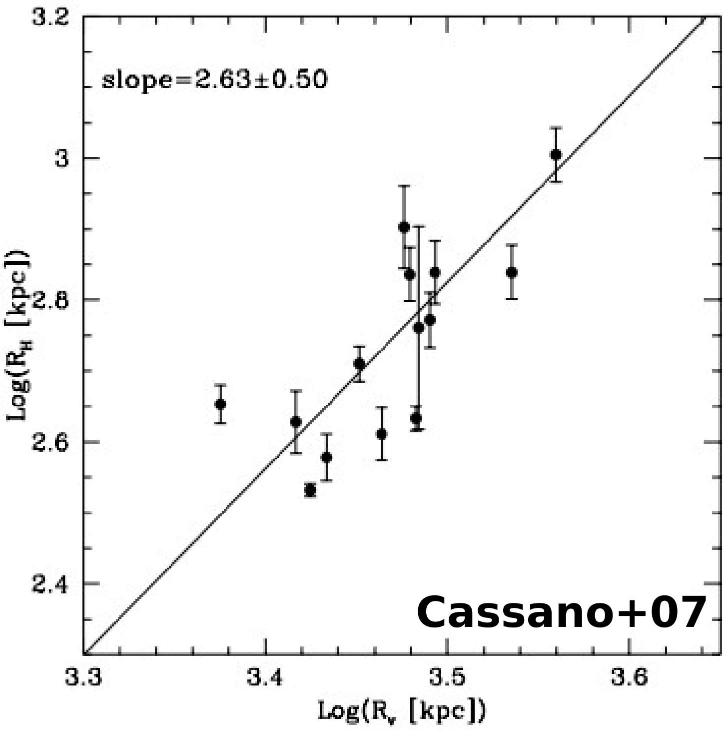

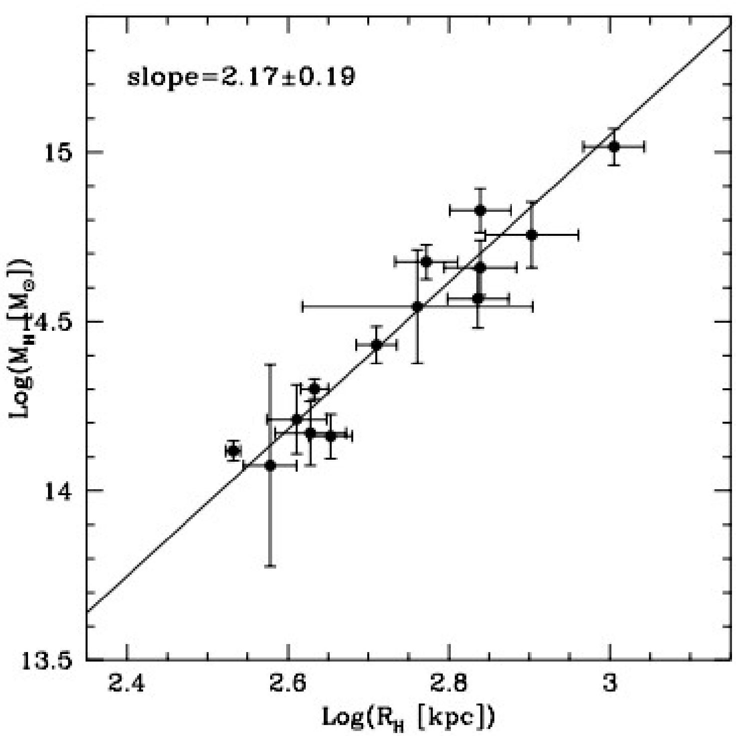

Radio re-scaling

$\gamma_{M,\exp}=2.10\pm0.35$

$\gamma_{M,\exp}=2.35\pm0.39$

	σ_{int}	Δ_σ	γ_M	$\Delta\,\gamma_M$	γ_z	$\Delta\,\gamma_z$
$I_{150MHz} \propto M^{\gamma_M}$	0.22	0.05	3.68	0.43	0 (fixed)	/
$I_{150MHz} \propto M^{\gamma_M}\ E_{z,\mathrm{fixed}}^{4/3}$	0.24	0.04	3.41	0.38	4/3 (fixed)	/
$I_{150MHz} \propto M^{\gamma_M}\ E_{z,\mathrm{fixed}}^{\alpha_M+4/3}$	0.28	0.04	2.85	0.43	4.10 (fixed)	/

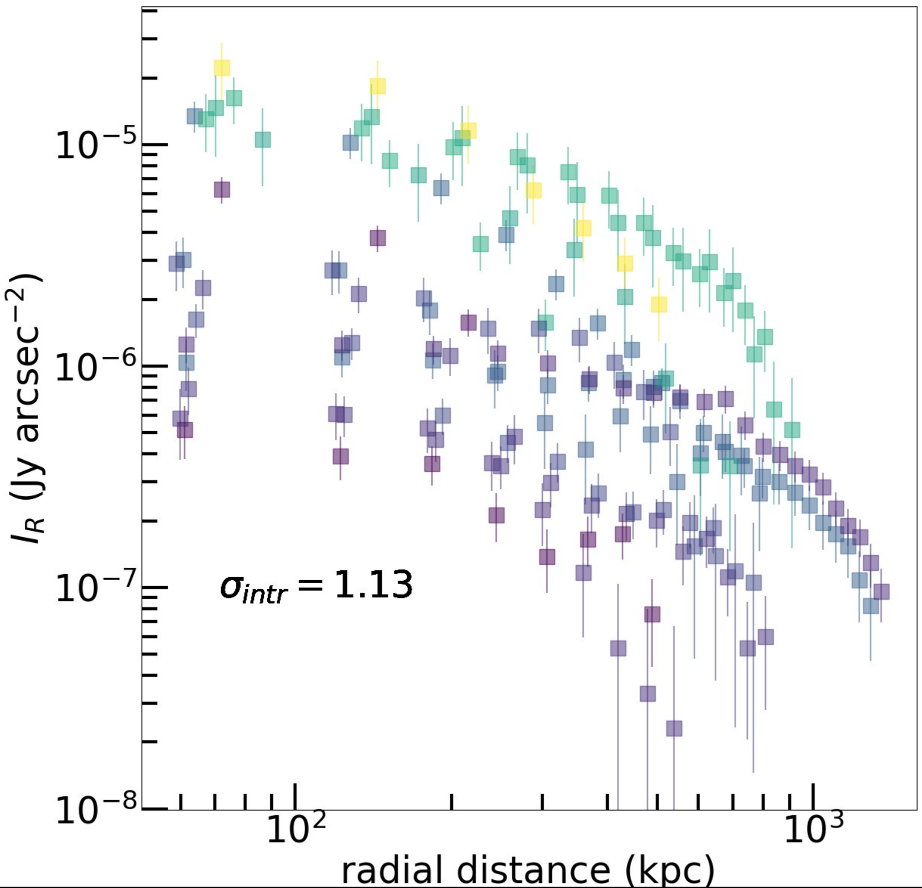

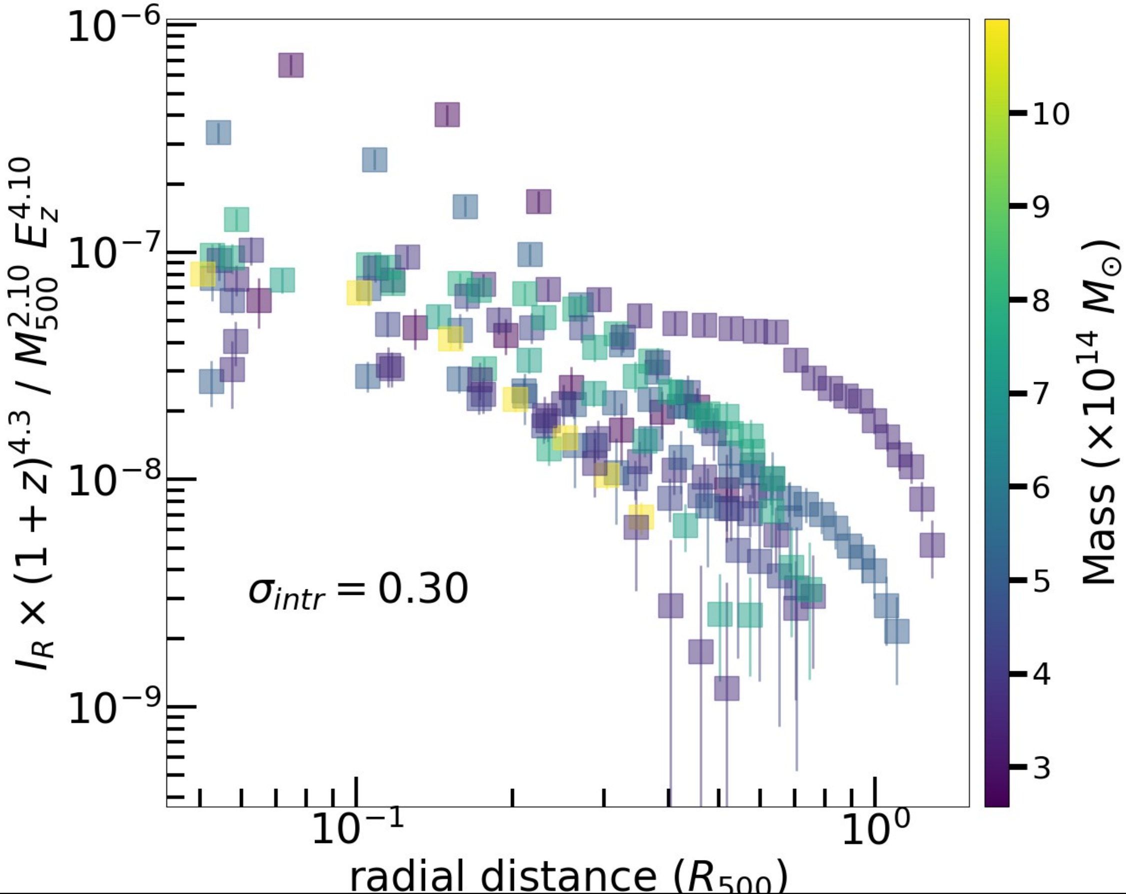

Radio re-scaling

	σ_{int}	Δ_σ	γ_M	$\Delta\,\gamma_M$	γ_z	$\Delta\,\gamma_z$
$I_{150MHz} \propto M^{\gamma_M}$	0.22	0.05	3.68	0.43	0 (fixed)	/
$I_{150MHz} \propto M^{\gamma_M}\ E_{z,\mathrm{fixed}}^{4/3}$	0.24	0.04	3.41	0.38	4/3 (fixed)	/
$I_{150MHz} \propto M^{\gamma_M}\ E_{z,\mathrm{fixed}}^{\alpha_M+4/3}$	0.28	0.04	2.85	0.43	4.10 (fixed)	/
$I_{150MHz} \propto (ME_z)^{\gamma_M}$	0.26	0.04	2.88	0.31	/	/

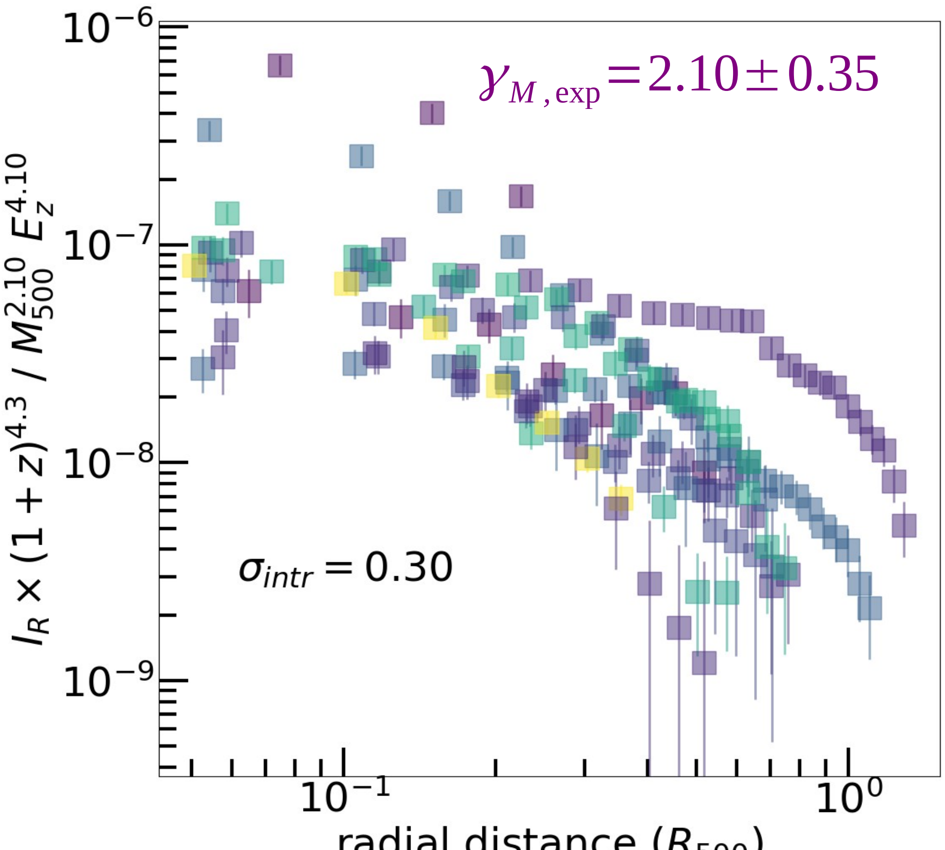

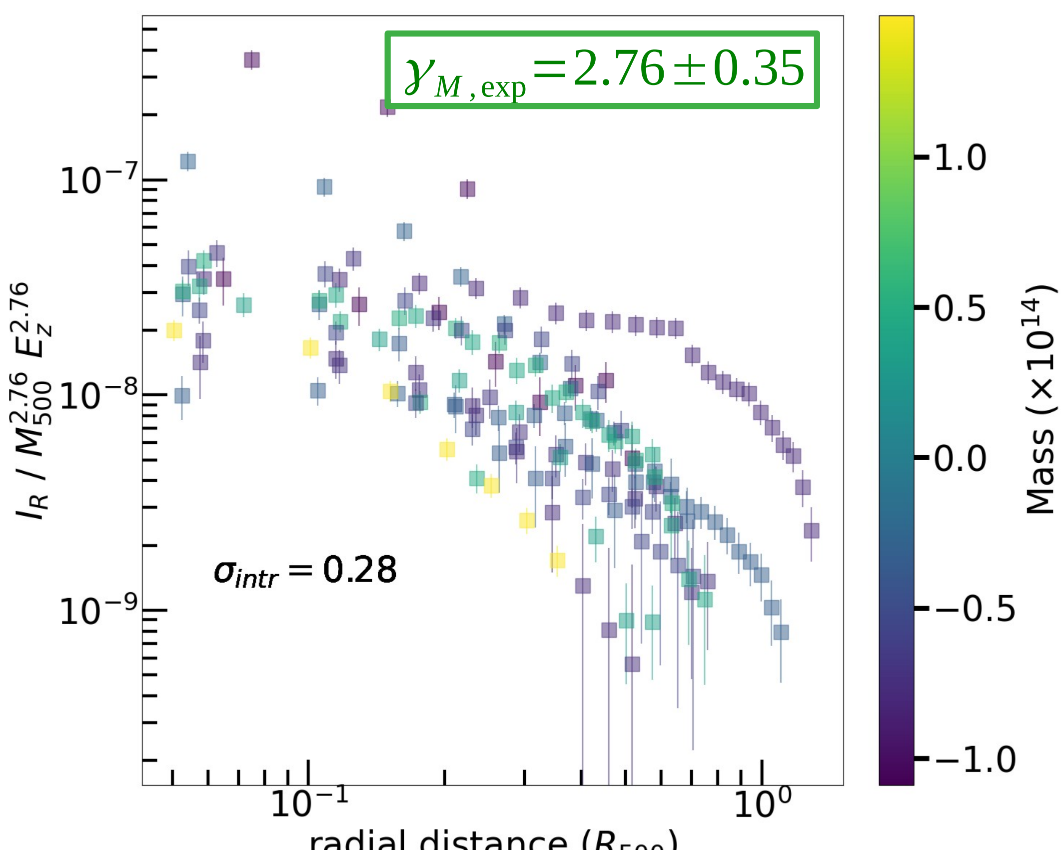

The role of B

$$P_R \propto \left(\frac{M}{M'}\right)^{\left(\frac{4}{3}-2b\right)} \left[1+\left(\frac{B_{CMB,0}}{B_{M'}}\right)^2 \frac{(1+z)^4}{(M/M')^{2b}}\right]^{-2}$$

$$\alpha_M = \frac{\log(P_1/P_2)}{\log(M_1/M_2)} = \psi(b, B_{M'})$$

Constrained from the observed P-M relation

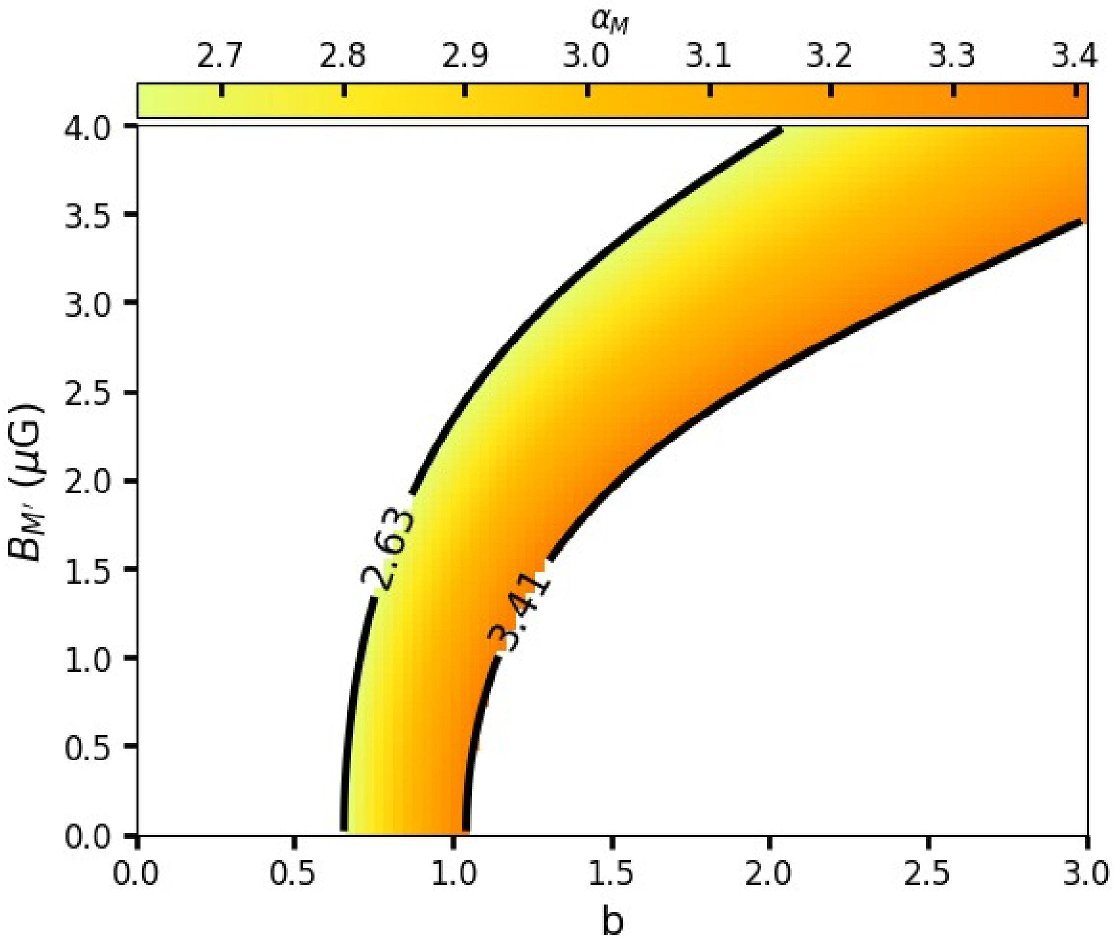

The role of B

$$P_R \propto \left(\frac{M}{M'}\right)^{\left(\frac{4}{3}-2b\right)} \left[1+\left(\frac{B_{CMB,0}}{B_{M'}}\right)^2 \frac{(1+z)^4}{(M/M')^{2b}}\right]^{-2}$$

$$\alpha_M = \frac{\log(P_1/P_2)}{\log(M_1/M_2)} = \psi(b, B_{M'})$$

Parameter	Prior	Best fit
b	$U(0,10)$	2.05 ± 0.36
$B_{M'}$	$U(0,10)$	2.53 ± 0.61
N	$U(0,10)$	2.82 ± 0.83
σ_{int}	$HC(0.5)$	0.95 ± 0.13
b (fixed)	/	1.33
$B_{M'}$	$U(0,10)$	2.11 ± 0.88
N	$U(0,10)$	3.20 ± 1.69
σ_{int}	$HC(0.5)$	1.04 ± 0.13

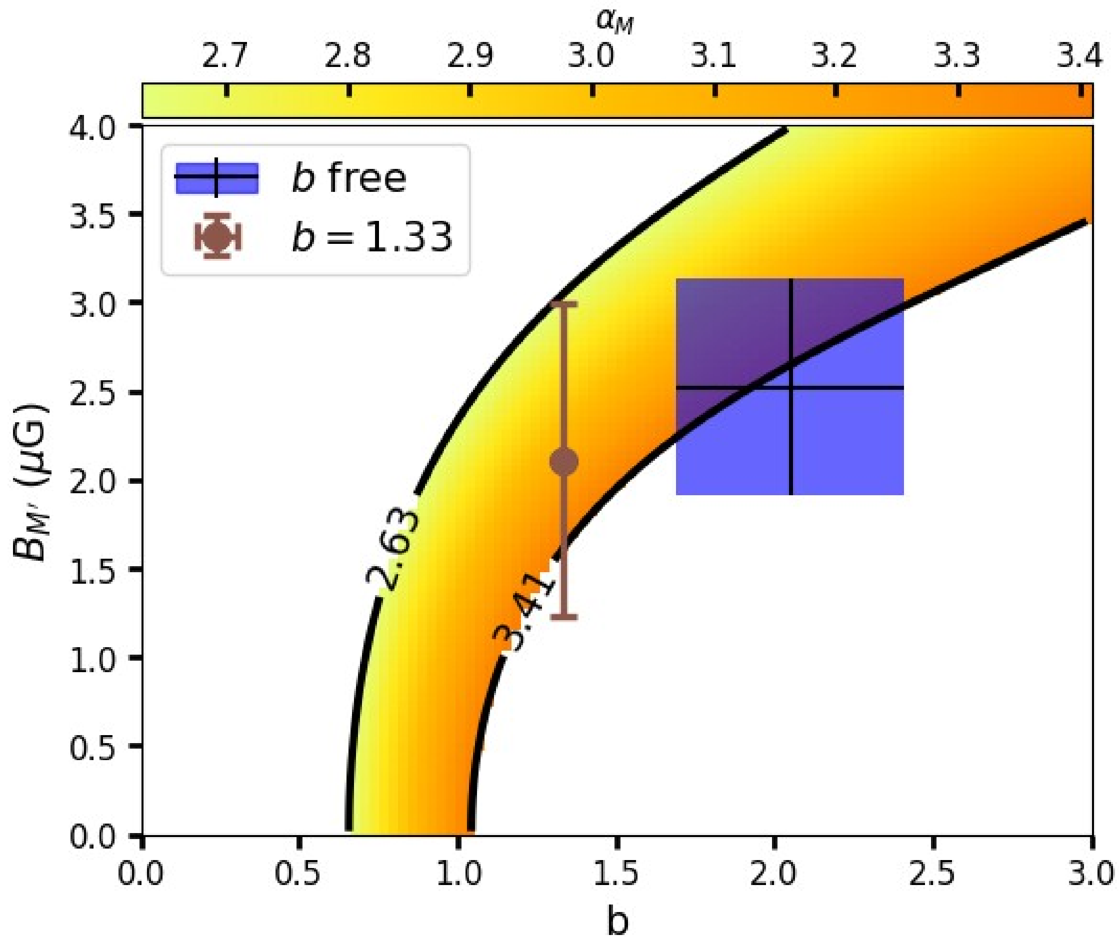

The role of B

$$P_R \propto \left(\frac{M}{M'}\right)^{\left(\frac{4}{3}-2b\right)} \left[1+\left(\frac{B_{CMB,0}}{B_{M'}}\right)^2 \frac{(1+z)^4}{(M/M')^{2b}}\right]^{-2}$$

$$\alpha_M = \frac{\log(P_1/P_2)}{\log(M_1/M_2)} = \psi(b, B_{M'})$$

+

Parameter	Prior	Best fit
b	$U(0, 10)$	2.05 ± 0.36
$B_{M'}$	$U(0, 10)$	2.53 ± 0.61
N	$U(0, 10)$	2.82 ± 0.83
σ_{int}	$HC(0.5)$	0.95 ± 0.13
b (fixed)	/	1.33
$B_{M'}$	$U(0, 10)$	2.11 ± 0.88
N	$U(0, 10)$	3.20 ± 1.69
σ_{int}	$HC(0.5)$	1.04 ± 0.13

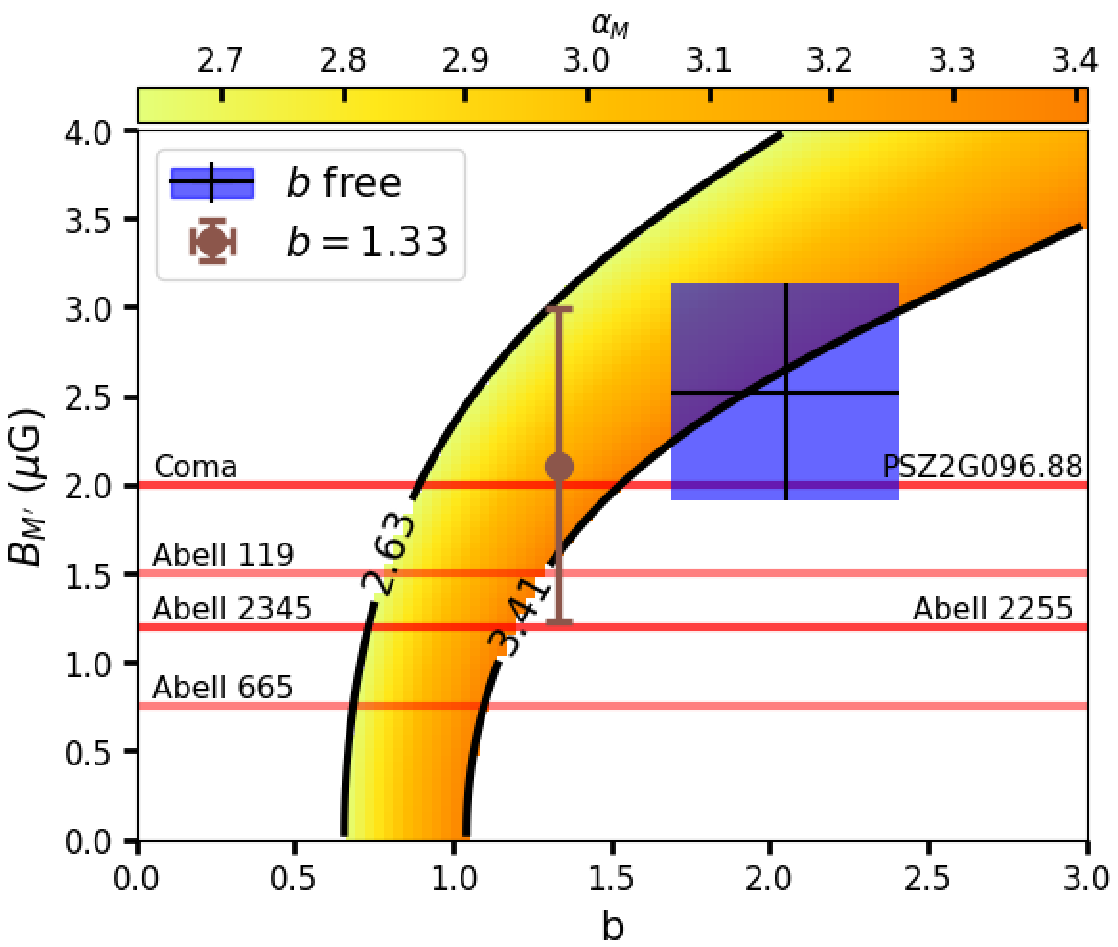

Backup slides

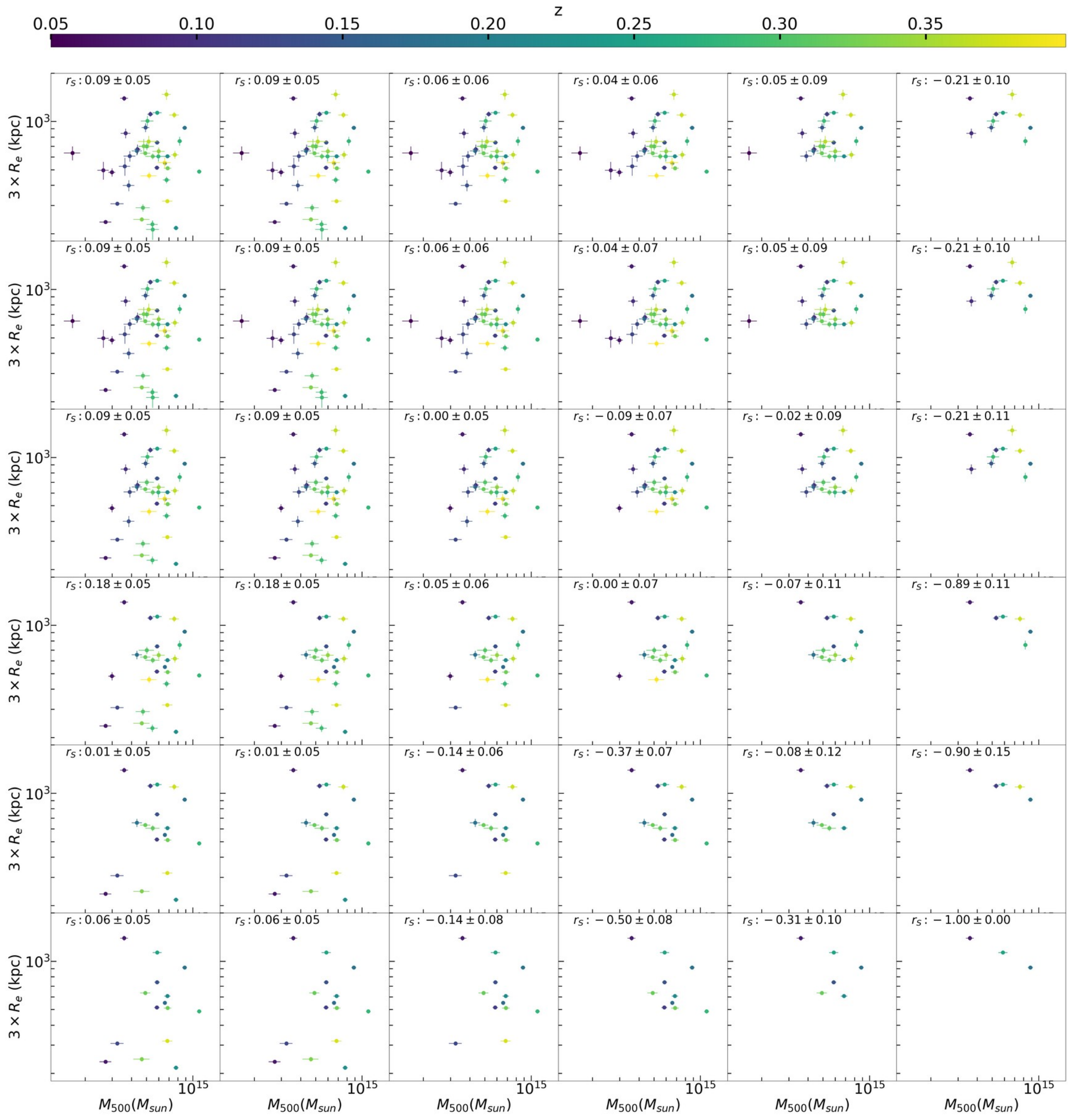

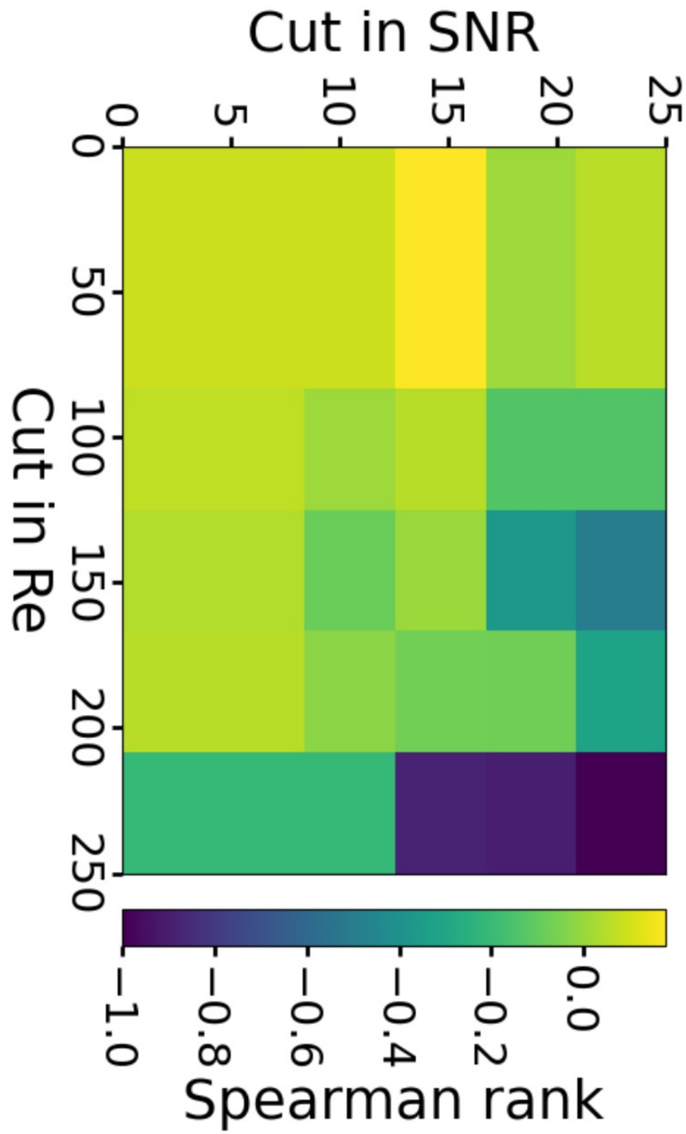

Backup slides

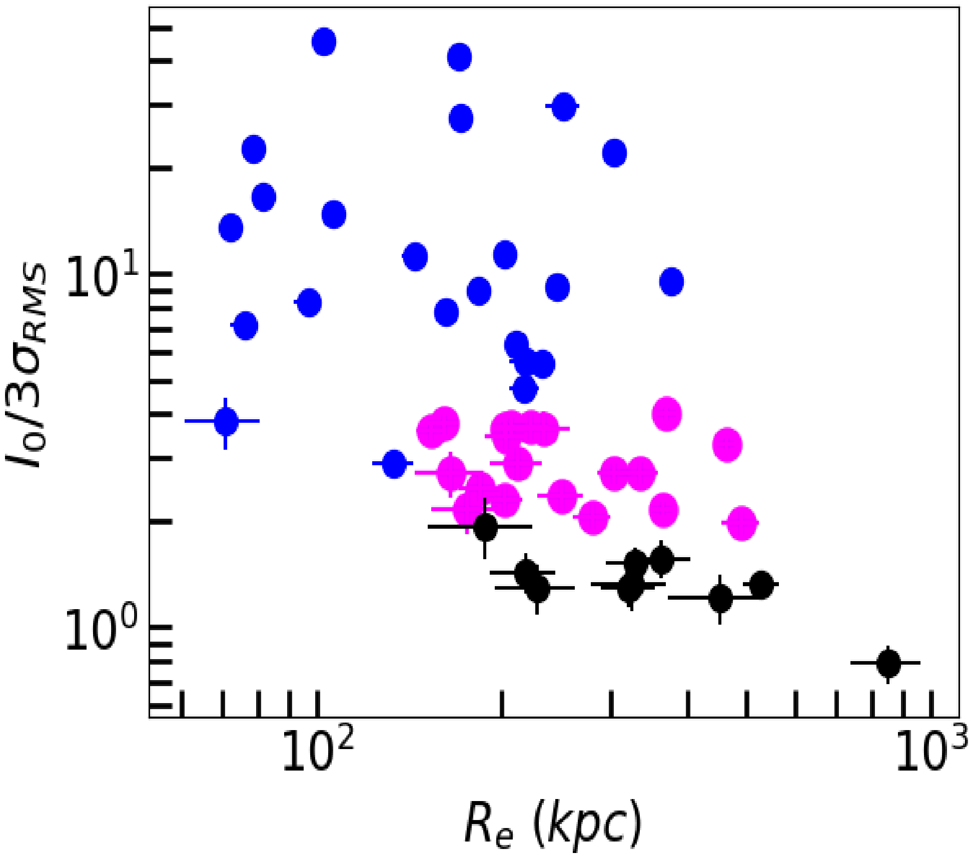

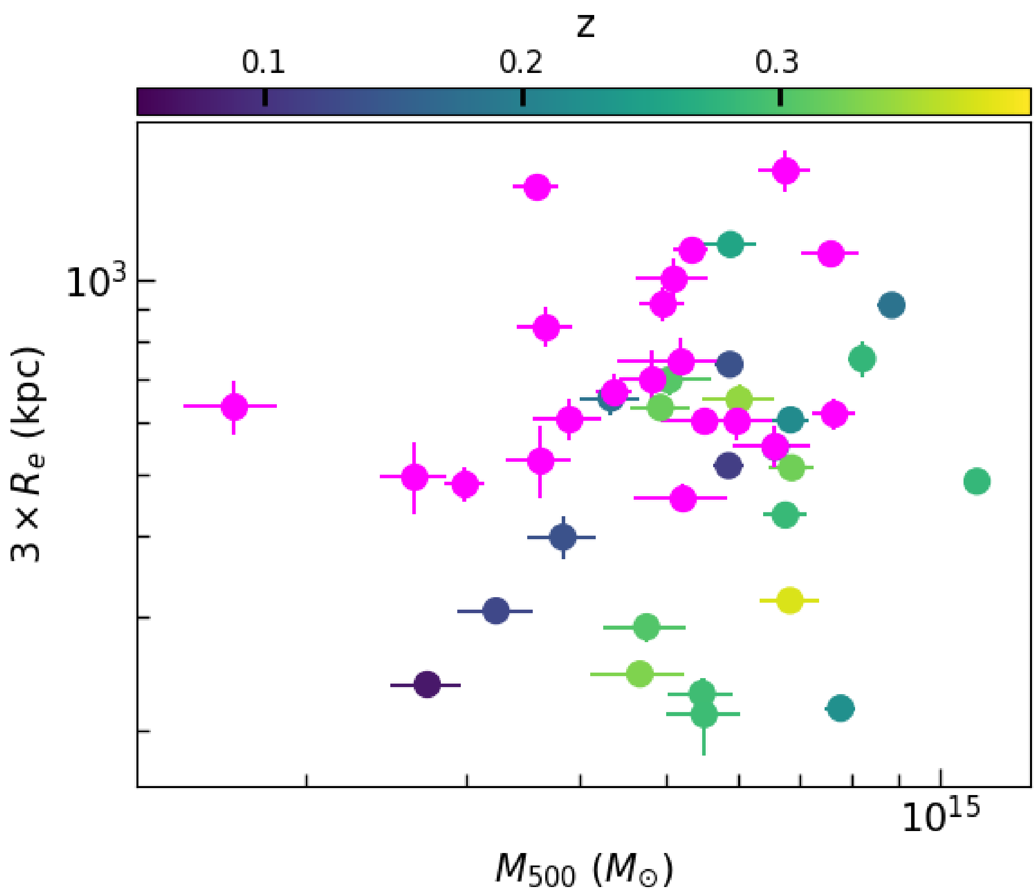

Backup slides

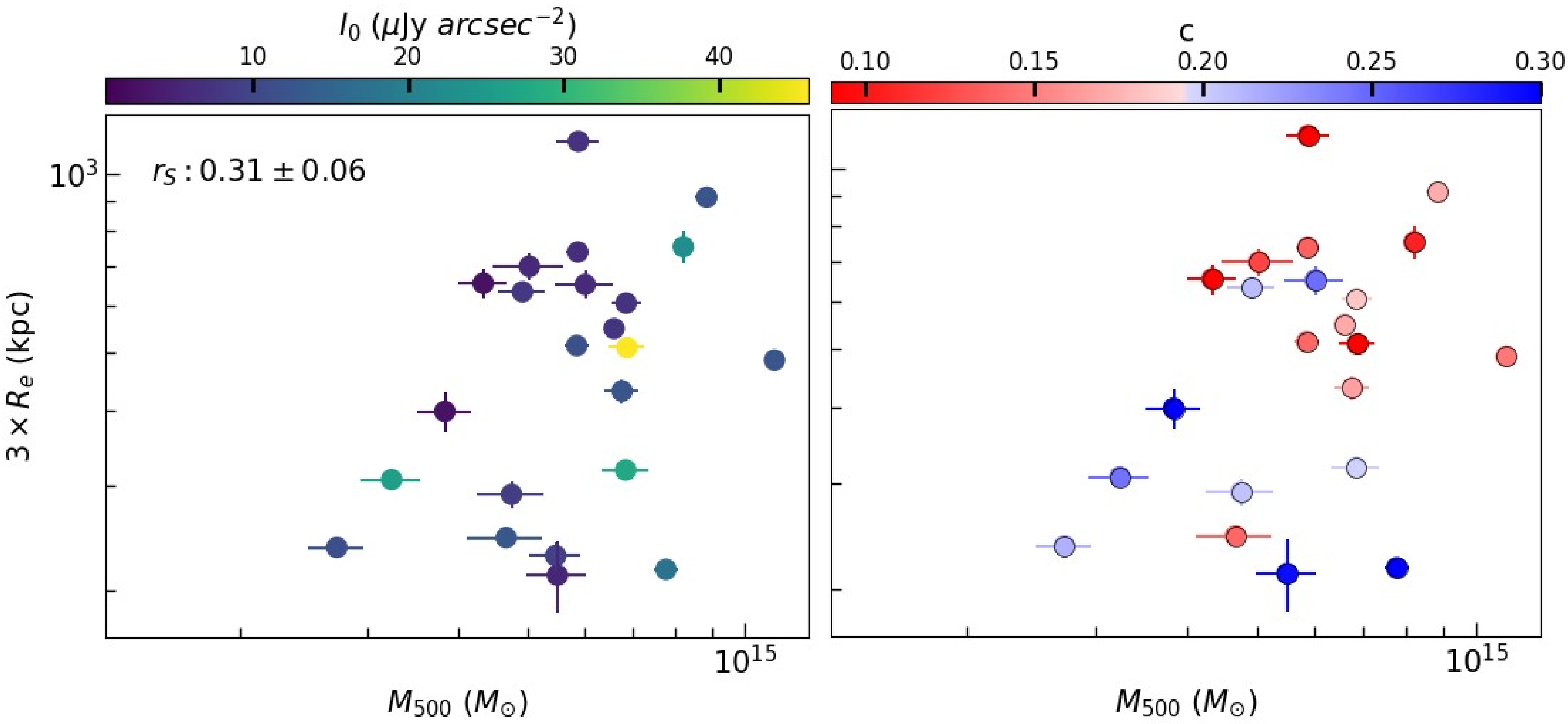

Backup slides